Science and Technology for Energy Transition **79**, 77 (2024)

https://doi.org/10.2516/stet/2024073

Available online at:
stet-review.org

Emerging Advances in Hybrid Renewable Energy Systems and Integration
Muhammad Zakarya, Santosh Tirunagari, Jinguang Han and Peiying Zhang (Guest Editors)

Regular Article | Open Access

Evaluating the contribution of demand response to renewable energy exploitation in smart distribution grids considering multi-dimensional behavior-driven uncertainties

Yahong Xing*, Changhong Meng, Wei Song, Haibo Zhao, Qi Li, and Ende Hu

Planning and Development Research Center, State Grid Shanxi Electric Power Company Economic and Technological Research Institute, Shanxi 030000, China

Received: 20 July 2024 / Accepted: 22 August 2024

Abstract. Demand Response (DR) is recognized as an efficient method for reducing operational uncertainties and promoting the efficient incorporation of renewable energy sources. However, since the effectiveness of DR is greatly influenced by consumer behavior, it is crucial to determine the degree to which DR programs can offer adaptable capability and facilitate the use of renewable energy resources. To address this challenge, the present paper proposes a methodological framework that characterizes the uncertainties in DR modeling. First, the demand-side activities within DR are segmented into distinct modules, encompassing load utilization, contract selection, and actual performance, to enable a multifaceted analysis of the impacts of physical and human variables across various time scales. On this basis, a variety of data-driven methods such as the regret matching mechanism is introduced to establish the analysis model to evaluate the impact of various factors on DR applicability. Finally, a multi-attribute evaluation framework is proposed, and the effects of implementing DR on the economic viability and environmental sustainability of distribution systems are examined. The proposed framework is demonstrated on an authentic regional distribution system. The simulation results show that compared to scenarios without considering uncertainty, the proposed method can fully consider the impact of DR uncertainty, thereby enabling a more realistic assessment of the benefits associated with DR in enhancing renewable energy accommodation for smart distribution grids. From the comparative analysis of new energy installation scenarios, with the integration of photovoltaic and wind power into the system, the presence of DR can increase the renewable energy consumption rate by 6.39% and 37.44%, respectively, and reduce the system operating cost by 1.37% and 3.32%. Through the comparative analysis of different load types, when DR is a shiftable load and a two-way interactive load, the renewable energy consumption rate increases by 20.57% and 26.35%, and the system operating cost decreases by 2.12% and 4.68%. In this regard, the proposed methodology, hopefully, could provide a reliable tool for utility companies or government regulatory agencies to improve power sector efficiency based on a refined evaluation of the potential for demand-side flexibility in future power grids incorporating renewable energies.

Keywords: Demand response, Demand-side behavior, Responsiveness potential, Smart grid.

Nomenclature

$P_{\mathrm{use},t}$	System's consumption capacity for renewable energy
$P_{\mathrm{sum},t}$	Total available power output of renewable energy generation
$P_{T,t}^{\mathrm{buy}}$	Power procured from the system assigned to period T
$P_{T,t}^{a.+}$	Upper spare capacity acquired in the auxiliary service market
$P_{T,t}^{a.-}$	Lower spare capacity acquired in the auxiliary service market
$P_{T,t}^{\mathrm{sl}}$	Load reduction
$P_{T,t}^{\mathrm{il}}$	Power reduction
C_1	Expense of buying power from the system
C_2/C_3	Cost factor of upper/lower spare capacity purchased
C_4/C_5	The cost factor of load/power reduction
$P_{k,t}^{\mathrm{il,rat}}$	Standard consumption or benchmark demand of interruptible loads
$P_{k,t}^{\mathrm{sl.rat}}$	Power demand of sheddable loads

* Corresponding author: edcftgbhu1234@163.com

Γ_k^I	Represents the customer's innate perception of the potential of the DR program
W_k^0	Availability payment
W_k'	Utilization payment
s_k'	Current action
s_k''	Different strategy

1 Introduction

Demand Response (DR), known to be a prominent feature of the smart grid, presents utilities with a groundbreaking approach to regulating power system operations through the utilization of customers' load demand flexibilities. According to the definition of reference [1], DR programs are designed to enable load-side customers to voluntarily modify their electricity use when the system is subjected to high market prices or emergencies. In this context, effective utilization of DR can sustain a crucial role in maintaining supply-demand equilibrium, which can impact the operational efficiency of upcoming power grids.

Among the numerous benefits of DR, a major aspect is its implication for renewable energy accommodation. In traditional power systems, planning or operation decisions mainly account for uncertainties stemming from the load side. In the future power system, renewable energy resources may be massively integrated with the global need to reduce carbon emissions [2]. However, renewable energy is intermittent in time and space [3]. It generates electricity intermittently and may account for a considerable percentage. As a consequence, the power system is likely to exhibit significant unpredictability on both the supply and demand sides [4]. Due to the above feature, it is challenging to fulfill efficient accommodation of renewable energies in the power system.

As a sort of market-based operation solution, incentive-based DR can encourage consumers to adjust power usage patterns, achieving comparable outcomes to supply-side resources [5]. As a virtual controllable asset, DR can be combined with a variety of power generation to efficiently mitigate the challenges posed by unpredictable renewable energy generation and load-demand disparities in power system operation [6], and improve the power grid's capacity to accommodate renewable energy.

At present, the application of DR in the power grid has been studied at home and abroad. Salehimehr *et al.* [7] develop a master-slave game trading model between system operators and load aggregators for DR, along with an optimization approach for multi-energy trading among diverse participants is presented. Norouzi *et al.* [8] investigated different load characteristics and types of DR programs. Reference [9] discusses the effects of time-of-use pricing on DR scheduling in the context of thermal energy storage, and based on the simulation outcomes, it can be inferred that combining energy storage with a time-of-use tariff can result in increased DR advantages specifically during peak hours. The load recovery effect associated with DR has been studied in reference [10] and it can be seen that in certain situations, the advantages of DR in terms of reliability may be substantially nullified by load recovery. Singh and Kumar [11] examine the involvement of various load resources to assist photovoltaic (PV) operation. References [12–14] prove that DR can help promote the application of renewable energy, enhance grid stability and reliability while lowering electricity costs. At the same time, Zhou *et al.* have conducted research on the DR flexibility of building energy systems, respectively from the aspects of system flexibility [15], collaborative optimization [16], and integrated application of renewable energy [17], and used machine learning methods to describe the demand side prediction of building energy system [18].

As for how to evaluate the contribution of DR in promoting the application of renewable energy in smart grid, Mehdi and Babak [19] present a security-constrained unit commitment framework that evaluates the effect of DR on power supply reliability. In reference [20], the influence of DR on the reliability of distribution networks is evaluated through Monte Carlo simulation techniques. Li and Wang [21] verify the feasibility of DR to promote renewable energy utilization by establishing various DR models. Yang *et al.* [22] calculate the contribution of DR to wind power usage under different incentive mechanisms based on a quantitative evaluation model. Amirhos *et al.* [23] recommend a multidimensional evaluation model that depends on an artificial neural network to implement a DR program. Shankar and Maurya [24] also propose a set of comprehensive evaluation methods for the valuation of DR benefits. In addition, reference [25] proposes a P2P optimization design method to increase DR Participation and promote renewable energy consumption.

Although considerable research efforts have been made so far, there are still some scientific gaps existed, which mainly arise from three of the following aspects:

Firstly, in the previous researches, the uncertainty of DR was not adequately considered. They commonly assumed that the utility companies possessed full knowledge about the demand responsivity of all the customers in the system; and all the DR resources were always accessible whenever envoked during the operation. These presumptions are generally applicable when DR is executed through a direct-control program, where customers got no option other than deciding whether to comply with DR requests from the grid. However, in reality, these assumptions may not always hold. If the study focuses on the non-direct control scenario, the circumstances will be quite different. In this case, users' responses to DR signals would be "voluntary," leading to unpredictable DR capacity that may significantly deviate from initial utility forecasts [11]. Consequently, the previously adopted assumption may no longer be justified in the non-direct control scenario.

Secondly, in current literature, the dynamic nature associated with DR activities has been largely disregarded [26–31], which imposes a great hurdle for their usage in real-world applications. In fact, for long-term analysis of smart-grid, since the time being considered is typically quite long (can take years), customers may modify their approach regarding their involvement (contractual setting) in the DR program dynamically during operation. In this case, the actual capacity for DR from the demand side becomes unstable and varies with customer decisions (i.e., the

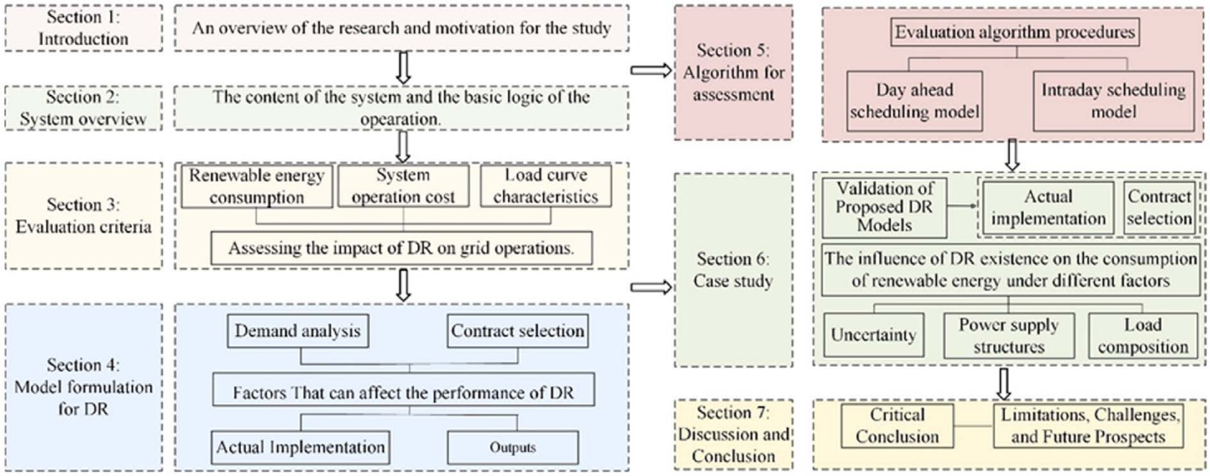

Fig. 1. Overall research roadmap of this paper.

willingness to participate in DR) over time. As such, neglecting the multi-time scale and dynamic feature in DR programs would lead to an unrealistic estimation on the benefits of DR program in the long run.

Finally, in the existing literatures, the currently adopted indicators for measuring the benefits of DR are relatively simplistic, which fail to fully capture the multidimensional value for DR implementation, especially concerning their implication for enhancing the utilization of renewable energy in smart grids.

To resolve the scientific gaps presented above, this study proposes a comprehensive DR modeling framework and applies it to the quantification of DR benefits in enhancing the utilization of renewable energy. As the novelty of this research work, this paper's proposed methodology can account for the impacts of uncertainties arising from both technical and human-related aspects within DR programs. Additionally, this paper explicitly incorporates the ambiguities of demand-side behaviors and their possible dynamics at multiple time-scales. To quantify the effect of DR on renewable usages scientifically, this paper also develops a systematic evaluation index system and algorithms.

In summary, compared with the related research, this study fully considers the uncertainty in the process of DR Implementation, and combines multi-time scales and dynamic characteristics to build a multi-dimensional benefit evaluation system for DR, the main contributions of this research can be summarized as follows:

The paper comprehensively models the multi-dimensional uncertainties of DR from a demand-side viewpoint, incorporate concurrently, within a same framework, both contingent and long-lasting dynamic ambiguity in non-direct control-based DR programs. This is unlike previous research which has only focused on examining temporary operational fluctuations of DR. This approach enables a more precise and practical assessment of the environmental and economic benefits of DR in real-world applications.

To create the DR model, the research integrates the strengths of analytic and data-driven approaches, making it generalizable and able to evaluate the DR attributes of various customer groups without implying any preconceived speculations about their behavior patterns or preferences.

A comprehensive multi-attribute assessment framework is proposed to explore the economic and environmental impacts of DR implementation in smart distribution systems. This framework relies on two key evaluation metrics: renewable energy utilization ratio and system operational cost. It also incorporates a multi-time scale optimal scheduling model, covering both day-ahead and intra-day scheduling.

The paper is structure as follows: Section 2 offers a system overview, Section 3 defines the evaluation criteria, Section 4 elaborates on the proposed DR modeling framework, Section 5 describes the algorithm used for the assessment, Section 6 makes a case study, and Section 7 provides a summary of the findings, concluding the research.

The overall research roadmap of this paper is shown in Figure 1.

2 System overview

This research is based on a smart distribution system comprising distributed renewable energy generation, distribution feeder lines, and responsive load demand from system customers. The utility company centrally manages all system modules.

In this study, it is assumed that each system customer is equipped with a smart load monitoring and management unit, allowing the system operator to remotely oversee and adjust their electricity consumption, such as the real-time switching of the customers' electrical devices.

Practically, customer load demand can be classified into different groups based on various criteria [32]. For instance, residential, industrial, and commercial loads can be distinguished according to the customer sector. Alternatively, curtailable, time-shiftable, and inelastic loads can be identified based on the characteristics of demand-side resources.

In a prospective smart distribution system integrating renewable sources and adaptable loads, a well-executed DR strategy can enhance renewable energy utilization and mitigate carbon emissions from the electricity sector, and improve system operations. For instance, during periods of low renewable energy output or high market prices, the system operator might reduce or delay demand from flexible loads to minimize energy procurement from the grid, reduce maintenance expenses, and mitigate carbon emissions. Conversely, when renewable energy output is high or market costs are low, the system operator may opt for DR to increase load demand, avoid curtailing renewable generation, and improve system economic performance.

In practical applications, DR can be acquired through price-based or incentive-based programs [33]. Price-based DR programs depend on time-variant pricing signals (such as time-of-use prices, real-time prices, etc.) to motivate customers to adjust their power demand pattern based on the current system's operational status. For example, real-time prices represent the marginal cost of supplying electricity to users within a specific time period, factoring in operational and foundational investment costs. Time-of-use prices involve segmenting a day into various periods based on the system's operational status, with each period charging electricity based on the average marginal cost of system operation. However, since these pricing signals are typically issued on an hourly basis, load demands are unable to closely track the stochastic power output of renewable energy generation and respond promptly. Therefore, price-based DR programs are less useful in addressing the challenge of renewable energy integration. Alternatively, incentive-based DR programs use a direct load control approach. In this approach, the system operator can directly monitor and manage electricity consumption on the demand side in compliance with the system's need for immediate response and performance. As a result, customer loads can promptly respond to system signals, promoting efficient renewable energy use.

However, incentive-based DR programs require users to change their initial consumption behaviors unexpectedly. Therefore, the degree to which the load controls impact customers who participate in such DR programs becomes a critical factor. In this sense, the impact of demand-side behaviors must be appropriately accounted for when assessing the contribution of incentive-based DR to renewable energy utilization.

During operation, when there is a timing mismatch between renewable energy generation and load demand, the system operator could invoke the DR potential of customers to maintain the secure, economical, and efficient operation of the system. To ensure the maximization of system benefits, the operator must determine the most suitable strategy for deploying DR under different scenarios, by optimization techniques. Then, the obtained DR commands are delivered to the customers via smart load monitoring and management unit and the targeted loads will be curtailed or shifted accordingly. After each time a DR is performed, the system operator records corresponding information about the DR capacity that is realized and pays a reward to the enrolled customer according to their bilateral agreement.

3 Evaluation criteria

Since this paper is mainly focused on assessing the impacts of DR in smart distribution grids, here, two evaluation indices are adopted, namely, the renewable penetration ratio η and grid operation cost C, to evaluate the influence of DR implementation on renewable energy utilization and the economic performance of the system, respectively.

The renewable penetration ratio η is defined as the quotient of the capacity of renewable energy that is utilized by the maximum generation output available, as given below:

$$\eta = \frac{\sum_{t=1}^{T} P_{\mathrm{use},t}}{\sum_{t=1}^{T} P_{\mathrm{sum},t}} \times 100\% \tag{1}$$

where $P_{\mathrm{use},t}$ is the capacity of renewable energy consumed by the system in time-period t; $P_{\mathrm{sum},t}$ represents the total available renewable energy power output in time period t (which depends on the meteorological conditions); T is the time horizon under study.

The system operating cost C consists of four items, which are the power purchase cost (in the day-ahead market), DR reward cost, loss-of-load cost, and the payment for purchasing ancillary services. The mathematical formulation is presented as follows:

$$C = \sum_{T=1}^{365} \left(\sum_{t=1}^{24} c_1 P_{T,t}^{\mathrm{buy}} + \sum_{t=1}^{24} c_2 P_{T,t}^{a,+} + \sum_{t=1}^{24} c_3 P_{T,t}^{a,-} + \sum_{t=1}^{24} c_4 P_{T,t}^{\mathrm{sl}} + \sum_{t=1}^{24} c_5 P_{T,t}^{\mathrm{il}} \right) \tag{2}$$

where $P_{T,t}^{\mathrm{buy}}$ is the power purchased from the system allocated to the period T at period t. To meet the active power demand under the negative new energy forecast deviation and disturbance accident, the power system must retain a certain number of operating reserve passengers in the day-ahead start-up mode and intra-day real-time generation planning. Scientific and reasonable setting of operating reserve capacity is the premise of ensuring the safe, the dependable and cost-effective operation of the power system. And when the upper reserve capacity is insufficient, it may lead to load cutting, and when the lower reserve capacity is inadequate, it may cause new energy abandonment such as wind abandonment and light abandonment. Therefore, it is necessary to set the spare capacity constraint. $P_{T,t}^{a,+}$ is the upper spare capacity purchased from the auxiliary service market for period T in a given time slot t during the day-ahead scheduling, $P_{T,t}^{a,-}$, $P_{T,t}^{\mathrm{sl}}$ and $P_{T,t}^{\mathrm{il}}$ are load reduction and power reduction. c_1 is the cost factor of purchased power from the system, c_2 and c_3 are the cost factor of upper and lower spare capacity purchased, c_4 and c_5 the cost factor of load reduction and power reduction, all in \$/Kw.

4 Model formulation for DR

4.1 Framework of DR modeling

To accurately estimate the DR, it is crucial to conduct a sophisticated analysis of the load characteristics and the associated uncertainties.

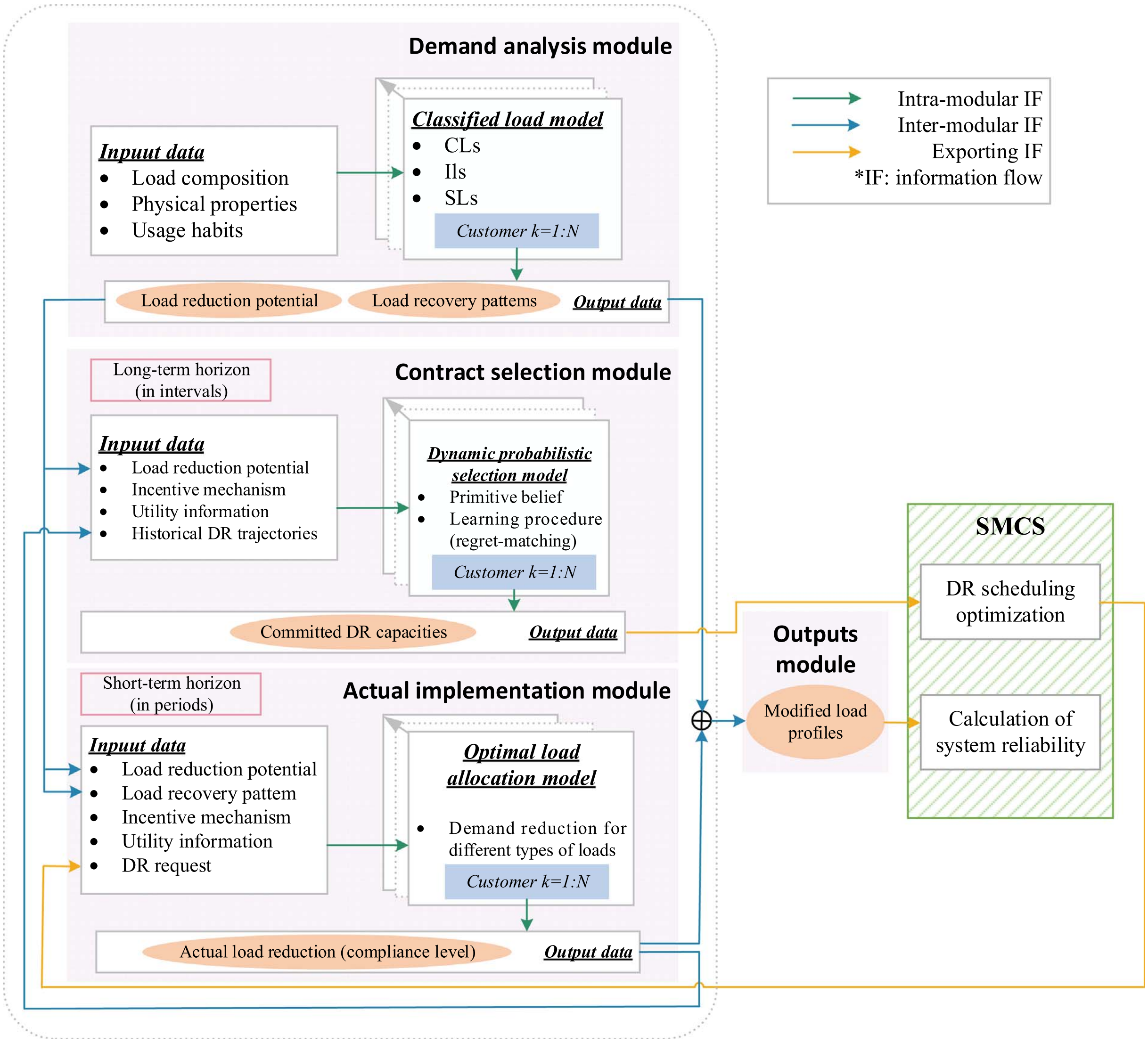

Fig. 2. Modelling framework of DR.

The two main categories of current methodologies used in DR modeling are analytical and data-driven [30]. The priori approach primarily analyzes the DR through the development of profit-oriented optimization models [26, 31]. Conversely, the data-driven methodology entails forecasting the DR capability through an analysis of historical customer behavior patterns [22, 34–36].

The most significant challenge posed by this scenario is the diversity in demand-side behavior. As the non-direct control scheme does not involve direct control, entities may exhibit diverse and potentially irrational behaviors in response to DR signals from the grid. However, it may be challenging for the system operator to obtain complete information regarding individual idiosyncrasies, such as their coherence and consumption preferences, etc. Furthermore, assuming such evidence is accessible, various unpredictable factors may impact the reliable responsiveness of users throughout the process. Due to these factors, system operators cannot adequately incorporate DR in practical settings using solely analytical methods.

In addition to the aforementioned challenges, in the context of long-term analysis, the dynamic nature of customer participation in DR programs results in potentially unstable available DR capacity within the system, but it may change as the demand-side participation progresses. According to the research conducted by [37], people's willingness to take part in DR programs is not solely determined by their preferences but is also influenced by factors like their previous payouts from the program. Unfortunately, the majority of existing DR modeling techniques fall short of accurately capturing the interconnected and evolving character of consumer behavior.

Considering the challenges discussed above, this paper recommends a comprehensive modeling approach for DR that addresses the above-addressed issues. As depicted in Figure 2, the system is made up of several components, that

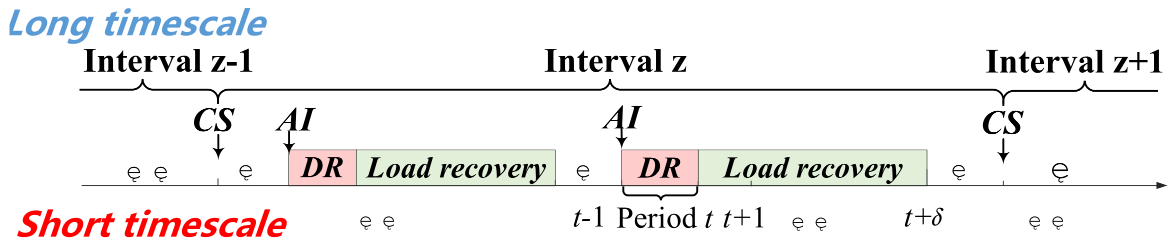

Fig. 3. Timescale for different modules.

model the various factors influencing DR at different time scales. The structural attributes of DR capabilities are analyzed in the demand analysis module, which provides a foundation for the overall research. Two distinct modules, contract selection and actual implementation assess the human-related factors of DR. The contract selection module models the decision-making process of individuals regarding DR subscription during the contract execution process, which typically encompasses an extended time frame. On the other hand, the actual implementation module evaluates the actual DR efficiency of customers during the immediate operating period, taking into account the restrictions imposed by strategic contract selection in the long run. The changing load profile brought on by DR under various operating conditions may be evaluated by integrating the outcomes from these components. The evaluation algorithm uses the data generated as the ultimate results of the framework to evaluate the DR.

Figure 3 illustrates the modeling of factors that exist on different time scales that have a significant impact on DR.

4.2 Demand analysis module

When considered from the material perspective, DR capability is primarily determined by the functional attributes of local requirements. Based on their degree of adaptability, electric loads can be broadly categorized as critical loads, interruptible loads, and shiftable loads [37].

Critical loads must run continuously under all circumstances. These loads typically include essential household appliances such as refrigerators, cooking equipment, and lighting fixtures. Given that the use of critical loads is often tied to the daily survival of individuals, they are designed to operate independently without any reliance on external signals or factors.

When referring to loads, interruptible loads are those whose expenditures may be reduced during system crises. Common examples of interruptible loads include heating, ventilation, and air conditioning systems. In the case of interruptible loads, when a power attenuation is commenced during a given time t, the resulting changing demand can be calculated as $P^{\mathrm{il}}_{k,t} = P^{\mathrm{il,rat}}_{k,t} - P^{\mathrm{il},-}_{k,t}$,where $P^{\mathrm{il,rat}}_{k,t}$ represents the standard consumption or benchmark demand of interruptible loads during period t.

Shiftable loads, or controllable electrical loads, can have their demands modified within a defined timeframe while adhering to overall energy constraints. Sheddable loads include plug-in electric heaters and water heaters. If a DR event starts while sheddable loads are operating, any energy saved during the DR event by reducing demand must be repaid by the customer after the event, based on the terms of their agreement.

To capture the behavior of both long-running loads and the associated uncertainties of sheddable loads, a vendor-neutral model is employed. This method utilizes two straight lines, as depicted in Figure 4, to characterize the demand reductions and restorations of sheddable loads. The ascending line represents the load increase following the DR event, while the declining line simulates the return of usage to the pre-DR level while taking into account the long-running process' waning influence [38].

Whenever a load reduction $P^{\mathrm{sl},-}_{k,tt}$ occurs, such as in period t, the restored demand in succeeding period t' ($P^{\mathrm{sl},+}_{k,tt}$) can be calculated distinctly as:

$$P^{\mathrm{sl},+}_{k,tt'} = \begin{cases} b^{\mathrm{sl}}_{k,0} + \varpi^{\mathrm{up}}_{k}(t'-t-1), t' \in \{t+1,\cdots,t+\delta^{\mathrm{pk}}_{k}\} \\ b^{\mathrm{sl}}_{k,1} - \varpi^{\mathrm{dw}}_{k}(t'-t-\delta^{\mathrm{pk}}_{k}), t' \in \{t+\delta^{\mathrm{pk}}_{k}+1,\cdots,t+\delta_{k}\} \\ 0, \qquad \text{else} \end{cases} \tag{3}$$

where:

$$b^{\mathrm{sl}}_{k,0} = \frac{\left[2P^{\mathrm{sl},-}_{k,t} + \varpi^{\mathrm{up}}_{k}(\delta^{\mathrm{pk}}_{k}-1)(\delta^{\mathrm{pk}}_{k}-2\delta_{k}) + \varpi^{\mathrm{dw}}_{k}(\delta_{k}-\delta^{\mathrm{pk}}_{k})^{2}\right]}{2\delta_{k}} \tag{4}$$

$$b^{\mathrm{sl}}_{k,1} = \frac{\left[2P^{\mathrm{sl},-}_{k,t} + \varpi^{\mathrm{up}}_{k}\delta^{\mathrm{pk}}_{k}(\delta^{\mathrm{pk}}_{k}-1) + \varpi^{\mathrm{dw}}_{k}(\delta_{k}-\delta^{\mathrm{pk}}_{k})^{2}\right]}{2\delta_{k}}. \tag{5}$$

And $\varpi^{\mathrm{up}}_{k}, \varpi^{\mathrm{dw}}_{k}, \delta_{k}$ and δ^{pk}_{k} are distinct characteristics that determine the form of the user's long-running structure.

The implementation of long-running loads by customers are typically uncontrolled, leading to uncertainties in the parameters described by equation (3) from the system operator's perspective. In practice, a load survey is often necessary to determine these parameter values, with statistical characteristics identified through long-term observation of customer load recovery behavior during DR events. For simplicity, this study assumes that $\varpi^{\mathrm{up}}_{k}, \varpi^{\mathrm{dw}}_{k}, \delta_{k}$, and δ^{pk}_{k} are normally distributed variables, these variables can be deduced through random sampling in the calculation. The demand for sheddable loads during DR can be represented by a combination of power reduction and payback, resulting in the following expression:

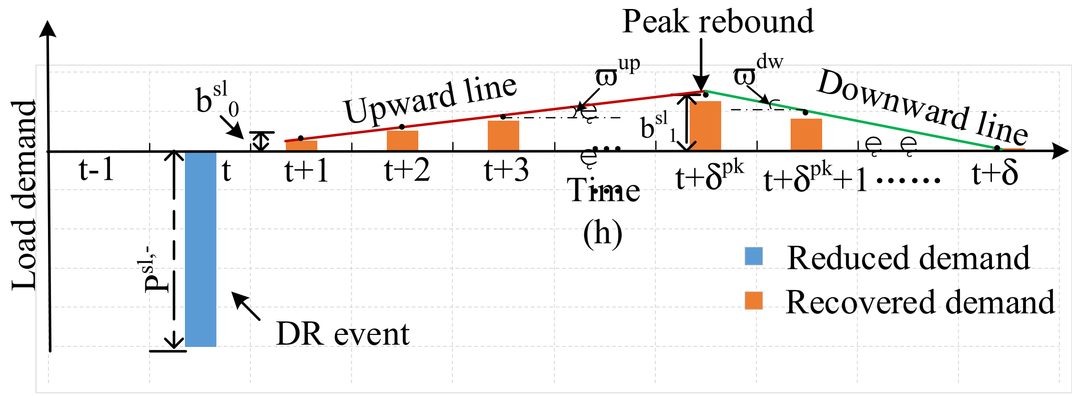

Fig. 4. Describing the demand recovery for controllable loads.

$$P^{\mathrm{sl}}_{k,t} = P^{\mathrm{sl,rat}}_{k,t} - P^{\mathrm{sl},-}_{k,t} + \sum_{t'=t-\delta_k}^{t-1} P^{\mathrm{sl},+}_{k,t't} \tag{6}$$

where $P^{\mathrm{sl,rat}}_{k,t}$ represents the power demand of sheddable loads at period t under typical circumstances (without DR).

4.3 Contract selection module

To represent demand-side actions during the contract selection phase, $\mathbf{\Omega}_D$ is identified as the group of system users or clients. For every user $k \in \mathbf{\Omega}_D$, suppose that all their potential actions/decisions for contract selection belong to a finite set $S_k = s^1_k, s^2_k, \ldots, s^M_k$, where each element in S_k is a percentage metric that represents the relationship between a user's contracted load reduction level and their overall DR capability which comprises $P^{\mathrm{il,rat}}_{k,t} + P^{\mathrm{sl,rat}}_{k,t}$. More, this paper defines a time-interval set $T_{\mathrm{cs}} = 1, 2, \ldots, z, \ldots$ to denote the contract terms or time horizons for making contract selection decisions. Therefore, each time-slot t in $z \in T_{\mathrm{cs}}$ can be represented as $t_z = \mathrm{mod}(t, z)$. Given the notations outlined above, the key issue in contract selection to tackle is determining the users' responsibility for selecting various actions in S_k for each interval $z \in T_{\mathrm{cs}}$.

To begin with, let's examine the scenario where no a priori information is available. Under such circumstances, as individuals typically have limited knowledge they are enrolled in, their selections of contract selection needs to rely solely on their judgment, which can be instinctual and subject. As a result, we can describe the likelihood of selecting each strategy $s'_K \in S_k$ through an empirical distribution $\Gamma^I_k = x^I_{k,0}(s'_K)$, wherein $x^I_{k,0}(s'_K)$ represents the probability value associated with s', and $\sum_{s'_K \in S_k} x^I_{K,0}(s'_K) = 1$ serves as a further specification or condition.

The variable Γ^I_k represents the customer's innate perception of the potential of the DR program. Specifically, it reflects the customer's inclination towards selecting different contract-level strategies based on their expectations of the rewards and benefits associated with DR participation. For instance, a customer with a favorable disposition towards DR may opt for high contract-level strategies, whereas those with reservations may prefer low-level strategies. It is important to mention that Γ^I_k is based on the customer's inherent tendency and stays constant throughout the DR program, without changing over time. This property makes Γ^I_k a useful tool for modeling the customer's decision-making behavior in DR programs.

While the aforementioned formulation serves as a viable method for modeling DR programs, it might not provide the precision necessary for conducting in-depth studies. This is because the model overlooks customers' learning capabilities, which can significantly affect their long-term decision-making. In real-world scenarios, customers can potentially predict the profitableness of DR programs derived from their past experiences and incorporate this information into their forthcoming decisions. Consequently, the likelihood of a customer choosing a specific contract selection strategy may not stay consistent throughout time, but instead, transform and vary. As a result, the customers' performance in the contract selection phase may not always conform to their innate pattern represented by Γ^I_k.

Thus, we will now elaborate on how to expand the model to integrate the scenario of a priori information. To calculate the remuneration gained by a customer for their DR actions during a given interval z, a benefit function U_k: $R_+ \to R$ is utilized. The configuration of U_k typically takes into account both the capacity and energy contribution of the DR program [39]. It is worth noting that some DR programs may also impose penalty policies for customers who fail to meet their contractual obligations. In such cases, a penalty charge G_k will be incurred, and its value will increase with the degree of violation committed by the customer [7].

Conversely, reducing (or shifting) the load can also create inconvenience to consumers. In DR research, such inconvenience is commonly expressed using a disutility function L_k: $R_+ \to R_+$, the input of this model is calculated in this way. Using the definitions provided above, the aggregate gain of the users (Wk) from participating in DR during interval z can be represented as follows:

$$W_k(s_{k,z}, P^{\mathrm{il},-}_{k,t_z}, P^{\mathrm{sl},-}_{k,t_z}) = W^0_k(s_{k,z}) + \sum_{t_z \in z} W'_k(P^{\mathrm{il},-}_{k,t_z}, P^{\mathrm{sl},-}_{k,t_z}) \tag{7}$$

$$W^0_k(s_{k,z}) = U_k(s_{k,z}, P^{\mathrm{il},-}_{k,t_z}, P^{\mathrm{sl},-}_{k,t_z}) - \sum_{t_z \in z} U'_k(P^{\mathrm{il},-}_{k,t_z}, P^{\mathrm{sl},-}_{k,t_z}) \tag{8}$$

$$W_k^{'}\left(P_{k,t_z}^{\mathrm{il},-}, P_{k,t_z}^{\mathrm{sl},-}\right) = \wp\left(U_k^{'}, G_k, L_k^{\mathrm{il}}, L_k^{\mathrm{sl}}\right). \tag{9}$$

The total customer payoff from DR participation in interval z, as shown in equation (7), comprises two components: the availability payment W_k^0 and utilization payment $W_k^{'} W_k^0$ is typically defined by the user's contractual level during interval z, represented by their contract selection decisions $s_{k,z}$ as represented by equation (8). Whereas, $W_k^{'}$ is determined by the users' actual performance throughout the operation $P_{k,t_z}^{\mathrm{il},-}$ and $P_{k,t_z}^{\mathrm{sl},-}$ which is a function of $U_k^{'}$, G_k, L_k^{il}, and L_k^{sl}, as shown in equation (9).

Typically, customers on the demand side have limited access to system information beyond their past observations and experiences, in normal situations. As a result, their decision-making in the contract selection phase often follows a "reflex-response" paradigm in praxeology [39]. Specifically, for every interval, customers may transition from their existing actions to alternative actions if they are perceived to yield higher payoffs. The likelihood of choosing an alternative strategy increases with its perceived superiority in terms of expected utility.

In this study, a theory based on behavioral economics principles is introduced, the regret-matching mechanism, to properly model the "reflex-response" effect exhibited by customers on the demand side. The initial design of the regret-matching mechanism was aimed at resolving the issue of local decision-making in scenarios where the available information about the environment is incomplete [34]. The distributed nature of the regret-matching mechanism makes it a suitable approach for modeling users' adaptive behaviors, such as those seen in the contract selection case explored here. Furthermore, the regret-matching mechanism relies on the premise of limited rationality in human decision-making, which enables it to model customer behavior more accurately in realistic settings. Based on these recognitions, this study develops the contract selection model with a regret-matching mechanism as follows.

For each interval $z \in T_{\mathrm{cs}}$, the regret-matching mechanism defines the regret of a customer $M_{k,z}(s_k', s_k'')$ for not selecting a different strategy $s_k'' \in s_k$ compared to the current action s_k' as:

$$M_{k,z}(s_k', s_k'') = \max\{E_{k,z}(s_k', s_k''), 0\} \tag{10}$$

$$E_{k,z}\left(s_k', s_k''\right) = \frac{1}{z}\left[\sum_{\tau\le z: s_{k,\tau}=s_k^{'}} W_k\left(s_{k,,\tau}''\right) - \sum_{\tau\le z: s_{k,\tau}=s_k^{'}} W_k\left(s_{k,\tau}'\right)\right]. \tag{11}$$

As observed, regret is determined by comparing a user's average payoff for a particular action, s_k', with the average payoff for a different action, $s_k'' \in s_k$, in the history up to z. The entire payoff for consumers, normalized $W_k(\cdot)$ over all the relevant intervals z is known as the average payoff. If the payoff for the alternate strategy s_k'' is lower than that of s_k', thus $M_{k,z}(s_k', s_k'')$ is 0.

To quantify regret, the system operator must understand the user's potential payoffs if they had taken different actions in the past, denoted as $W_k(s_{k,\tau}'')$ in equation (11). However, in practice, obtaining such information from users may not always be feasible, rendering equation (10) inapplicable.

To address this issue, a conversion of the formulation $E_{k,z}$ is necessary. In the context of prolonged research, if the possibility of selecting the strategy s_k'' is a times of strategy s_k', then based on the principle of the law of large numbers, the frequency of s_k'' happening will be a times higher than that of s_k'. Consequently, the estimated total payoff for intervals where s''_k is chosen can be calculated by increasing the reward s_k' by a factor of $1/a$. The alternative method of the s_k', denoted as the first expression in (11), can be rephrased as:

$$\sum_{\tau\le z: s_{k,\tau}=s_k'} W_k(s_{k,\tau}'') = \sum_{\tau\le z: s_{k,\tau}=s_k''} x_{k,\tau}\left(s_k'\right) \cdot W_k(s_{k,\tau}')/x_{k,\tau}(s_k'') \\ x_{k,\tau}(\cdot) \tag{12}$$

where $x_{k,\tau}(s_k)$ indicates the likelihood of s_k to be selected at $\tau \le z$. In practical applications, this system operator can easily calculate the value of $x_{k,\tau}(\cdot)$ using past customer data, making equation (12) manageable for the system operator.

Using the refined regret measure in regret-matching mechanism, the tendency of customers $k \in \boldsymbol{\Omega}_D$ towards their decisions in contract selection can be defined. Then the probability distribution $\boldsymbol{\Gamma}_{k,z+1}^{\mathrm{B}}$ represents the possibility of the user selecting policy $s_k'' \in s_k$ at $z + 1$.

$$\boldsymbol{\Gamma}_{k,z+1}^{\mathrm{B}} = \begin{cases} x_{k,z+1}^B(s_k') = \min\left\{\dfrac{1}{\gamma} M_{k,z}(s_k', s_k''), \varsigma\right\} \\ x_{k,z+1}^B(s_k') = 1 - \displaystyle\sum_{s_k'\in S_k: s_k''\ne s_k'} x_{k,z+1}^B(s_k'') \end{cases} \tag{13}$$

where $x_{k,z+1}^B(s_k')$ and $x_{k,z+1}^B(s_k'')$ represents the likelihood that a user will choose a strategy s_k' and s_k'', respectively; the scaling factor γ is accompanied by a small predetermined constant, denoted by ς, this ensures ensure the total suggested probability is not greater than 1.

Equation (13) shows that a client has two options at each interval z: to continue adopting the identical strategy employed during the previous time period $z - 1$ s_k' or turn to choose a different action, or shift into a different action, $s''_k \in S_k, s''_k \ne s'_k$, with probabilities that are directly correlated to the level of regret associated with each option, $M_{k,z}(s_k', s_k'')$. Furthermore, selecting ζ as a minimum makes sure that every strategy S_k has a positive probability of being selected, which aligns with the fundamental concept of reflex-response. As a result, the proposed model in equation (13) is in complete agreement with the reflex-response principle.

Until now models have been constructed for customer decision-making in the context of contract selection, both with and without the availability of a priori information. However, in reality, individuals may not always conform to either of these models, as they may not be completely adaptable or entirely obstinate. As a result, their actual behavior at the contract selection can fall somewhere between the estimates of the two models. To address this issue, the distributions $\boldsymbol{\Gamma}_k^I$ and $\boldsymbol{\Gamma}_k^B$ can be combined as suggested above, the customer contract selection model is determined as follows:

$$\Gamma_{k,z+1} = \begin{cases} x_{k,z+1}(s''_k) = (1-\lambda_k)\min\left\{\frac{1}{\gamma}M_{k,z}(s'_k, s''_k), \varsigma\right\} + \lambda_k x_{k,0}(s''_k) \\ x_{k,z+1}(s'_k) = 1 - \sum_{s''_k \in S_k : s''_k \neq s'_k} x_{k,z+1}(s''_k) \end{cases}. \tag{14}$$

The final probability of a customer selecting an action $s''_k(x_{k,z+1}(s''_k))$ represented as a combination of two probability vectors, as demonstrated in equation (14). The initial value, with weight $1-\lambda_k$, captures the outcome of users' compliance, whereas the later value, with weight λ_k, indicates the influence of customers' inherent preferences on their choices. The weighting coefficient $0 \leq \lambda_k \leq 1$ determines the significance of the customer's past experiences. In practice, the system operator must collect information about users' contract selection actions s_k in the past to determine the value λ_k. The disparities between the data that was observed and the estimation outcomes produced by the two-component models can be calculated using statistical techniques. The obtained distances can serve as indicators of the 'closeness' of users' behavior patterns to the Γ_k^I and Γ_k^B distributions. Through the normalization of the computation of these distance measures, the value λ_k can be quantified. Detailed procedures for estimating λ_k are provided in Algorithm 1.

Algorithm 2 can be used by the system operator to update and calculate $\Gamma_{k,z}$, $k \in \Omega_D$ at interval $z \in T_{\mathrm{cs}}$ during estimation. Once calculated, the contract selection module can use the results to determine the user's DR capacity during a specific time period t_z based on equation (15) for a given

$$P^{\mathrm{av}}_{k,t_z} = s'_{k,z}\left(P^{il,\mathrm{rat}}_{k,t_z} + P^{sl,\mathrm{rat}}_{k,t_z}\right). \tag{15}$$

4.4 Actual implementation module

The implementation module specifically outlines the decision-making challenges customers face upon receiving DR calls, compelling them to adapt their energy consumption habits dynamically in response to operational requests. To do so, let P^{drr}_{k,t_z} represent the decrease in demand mandated by system operator at time-slot t_z, the benefit function follows U'_k and G_k, U'_k and G_k are inverse functions that depend on the consumers' reactions $P^{\mathrm{il},-}_{k,t_z} + P^{\mathrm{sl},-}_{k,t_z}$ and its departure from the level requested $P^{\mathrm{drr}}_{k,t_z} - P^{\mathrm{il},-}_{k,t_z} - P^{\mathrm{sl},-}_{k,t_z}$, respectively. Furthermore, the cost functions L^{il}_k and L^{sl}_k represent the costs of inconvenience imposed by DR, and these costs escalate with the extent of response and frequency of occurrence among customers, respectively.

Using the functions presented above, it is possible to define the total payoff a customer receives for modifying their demand at a time slot t_z (W'_k). This payoff is calculated by taking the weighted gap between expected revenues from the consumer and the cost of their suffering.

Algorithm 1. Estimating the weighting coefficient for contract selection.

Input: Historical contract selection decisions of customers $S_k = \{s_{k,1}, s_{k.2} \cdots, s_{k,N}\}$;

Probability distribution Γ_k^I and Γ_k^{B}

Output: The weighting coefficient $\lambda_k, \forall k \in \Omega_D$

Compute the expectation value of $\mathrm{s_k}$ and form a time series $S_k^{hs} = \{\overline{s}_{k,1}, \overline{s}_{k.2} \cdots, \overline{s}_{k,N}\}$.

Compute the expectation of estimated data provided by Γ_k^I and Γ_k^{B} and form the time-series $S_k^I = \{\overline{s}_{k,1}^I, \overline{s}_{k,2}^I \cdots, \overline{s}_{k,N}^I\}$ and $S_k^B = \{\overline{s}_{k,1}^B, \overline{s}_{k,2}^B \cdots, \overline{s}_{k,N}^B\}$.

Calculate the Euclidean distances $d_k^I = \sqrt{\Sigma_{n=1}^N (\overline{s}_{k,n}^I - \overline{s}_{k,n})^2}$ and $d_k^B = \sqrt{\Sigma_{n=1}^N (\overline{s}_{k,n}^B - \overline{s}_{k,n})^2}$ between S_k^{hs} to S_k^I and S_k^B, respectively.

Determine λ_k by normalizing d_k^I and d_k^B according to $\lambda_k = d_k^B / (d_k^I + d_k^B)$ and $1 - \lambda_k = d_k^I / (d_k^I + d_k^B)$.

Export the outcome of λ_k.

$$\begin{aligned} W'_k(P^{\mathrm{il},-}_{k,t_z}, P^{\mathrm{sl},-}_{k,t_z}) = \omega_k[&U'_k(P^{\mathrm{il},-}_{k,t_z} + P^{\mathrm{sl},-}_{k,t_z}) + \rho_k P^{\mathrm{il},-}_{k,t_z} \\ &- G_k(P^{\mathrm{drr},-}_{k,t_z} - P^{\mathrm{il},-}_{k,t_z} - P^{\mathrm{sl},-}_{k,t_z})] \\ &- (1-\omega_k)[L^{\mathrm{il}}_k(P^{\mathrm{il},-}_{k,t_z}) + L^{\mathrm{sl}}_k(P^{\mathrm{sl},-}_{k,t_z})] \\ &P^{\mathrm{drr}}_{k,t_z} \\ &t_z. \end{aligned} \tag{16}$$

In equation (16), ρ_k presents the price of retail electricity while $\rho_k P^{\mathrm{il},-}_{k,t_z}$ indicates the amount by which the user's electricity bills are reduced as a result of demand reduction. The weighting coefficient $0 \leq \omega_k \leq 1$ specifies the individual's preference for incentive rewards versus comfort at a time-slot t_z. In the context of the program, the degree to which users comply with DR signals is often uncertain. This uncertainty is captured by the variable ω_k which a probability distribution can be used to describe $\psi(\omega_k)$.

In reality, the system operator does not know the form and coefficients of $\psi(\omega_k)$, and they must be discovered from client history data. In this research, a non-parametric kernel density-based approach [35] has been employed to achieve this. In contrast to conventional techniques, non-parametric kernel density-based approach does not depend on assumptions about the parameters or a priori knowledge of the variables. As a result, non-parametric kernel density-based approach is capable of fitting any probability distribution shape and can therefore identify various customer behavior patterns in real-world situations. The detailed procedures for determining $\psi(\omega_k)$ with non-parametric kernel density-based approach are outlined in Algorithm 3.

Random sampling from $\psi(\omega_k)$ is the process that defines the value of ω_k. The anticipated customer response level

Algorithm 2. The algorithm used for deriving the distribution $\Gamma_{k,z}$.

Input: Set of contract selection strategies S_k ; payoff function W_k ;

Empirical distribution Γ_k^I ;

Historical DR records $s_{k,\tau}, P_{k,t_\tau}^{il,-}, P_{k,t_\tau}^{sl,-}, P_{k,t_\tau}^{drr}, \forall\tau < z$

Output: The probability distribution $\Gamma_{k,z}, \forall k \in \Omega_D$

Pick a first course of action $s_k^{'}$ from S_k and set $\tau = 1$

Loop

t=1

Repeat

Check to see if user k has a DR in slot t

If yes, retrieve the data of $P_{k,t_\tau}^{il,-}$ and $P_{k,t_\tau}^{sl,-}$, and record

Else, continue

t ← t+1

Check if $t \in \tau$

If yes, go back to 4)

Else

for $\forall s_k^{''} \in S_k \mid s_k^{''} \neq s_k^{'}$ do

Quantify users payoff W_k under $s_k^{''}$ and $s_k^{'}$, Eq. (7)

Compute the regret measure $M_{k,\tau}(s_k^{'}, s_k^{''})$ Eq. (10)

End for

Determine $\Gamma_{k,\tau}^{B}$ according to Eq. (13)

Check whether $\tau = z$

If yes, combine $\Gamma_{k,\tau}^{B}$ and Γ_k^I to derive $\Gamma_{k,z}$ based on Eq. (14)

Else, $\tau \leftarrow \tau + 1$

Go back to 2)

End loop

(load reduction) $k \in \Omega_D$ at time t_z can be calculated by resolving the subsequent optimization issue:

$$\underset{P_{k,t_z}^{\mathrm{il},-}, P_{k,t_z}^{\mathrm{sl},-}}{\text{maximize}} \; W_k' \tag{17}$$

$$0 \leq P_{k,t_z}^{\mathrm{il},-} \leq P_{k,t_z}^{\mathrm{il,rat}} \tag{18}$$

$$0 \leq P_{k,t_z}^{\mathrm{sl},-} \leq P_{k,t_z}^{\mathrm{sl,rat}} \tag{19}$$

$$\begin{array}{c} P_{k,t_z}^{\mathrm{il},-} + P_{k,t_z}^{\mathrm{sl},-} \leq P_{k,t_z}^{\mathrm{drr}} \\ P_{k,t_z,t'}^{\mathrm{sl},+} \end{array}. \tag{20}$$

Equations (18) and (19) are employed here to guarantee that the power reduction obtained from interruptible loads and shiftable loads remains within their available capacity during the specified period. Additionally, since emergency DR is implemented only at the behest of the system operator, it is imperative to ensure that the customer's total DR level does not exceed the required amount. Constraint equation (20) is formulated for this very purpose.

Algorithm 3. Estimating the weighting coefficient for actual implementation.

Input: Benefit/disutility functions $U_k^{'}, G_k, L_k^{\mathrm{il}}, L_k^{\mathrm{sl}}$;

Historical DR trajectories, $P_{k,t_z}^{\mathrm{il},-}, P_{k,t_z}^{\mathrm{sl},-}, P_{k,t_z}^{\mathrm{drr},-}$

Output: The probability distribution $\Psi(\omega_k)$, $\forall k \in \Omega_D$

Formulate users ' decision-making for actual implementation into a Lagrange function

$$V\left(P_{k,t_z}^{\mathrm{il},-}, P_{k,t_z}^{\mathrm{sl},-}, \eta\right) = W_k^{'}(P_{k,t_z}^{\mathrm{il},-}, P_{k,t_z}^{\mathrm{sl},-}) + \eta\, \mathrm{h}_k(P_{k,t_z}^{\mathrm{il},-}, P_{k,t_z}^{\mathrm{sl},-})$$

, where $\mathrm{h}_k(\bullet)$ represents the constraints and η is the Lagrangian multiplier (vector), $\eta \neq 0$.

Derive the Karush-Kuhn-Tucker optimality conditions for function, *i.e.*, $\partial \mathrm{V}_k / \partial P_{k,t_z}^{\mathrm{il},-} = 0$, $\partial \mathrm{V}_k / \partial P_{k,t_z}^{\mathrm{sl},-} = 0$, and $\eta\, \mathrm{h}_k(P_{k,t_z}^{\mathrm{il},-}, P_{k,t_z}^{\mathrm{sl},-}) = 0$. The set of equations obtained is denoted as P'.

For each historical data point, defined as $P_k^{\mathrm{hdr}} = \left(P_{k,t_z}^{\mathrm{drr},-}, P_{k,t_z}^{\mathrm{il},-}, P_{k,t_z}^{\mathrm{sl},-}\right)$ do

Substitute the data set P_k^{hdr} into equations P' and determine ω_k by solving P'.

Record the calculations ω_k.

End for

Estimate k) by utilizing a nonparametric technique based on kernel density and export the result

Since the equations (17)–(20) is a nonlinear programming problem with linear constraints, it can be solved using method [38]. Equations (17)–(20) may be solved using the interior point method [38], given that the problem involves nonlinear programming subject to linear constraints. The model's calculation will show the ideal level of power curtailment concerning interruptible loads and shiftable loads from the viewpoint of a client, $P_{k,t_z}^{\mathrm{il},-}$ and $P_{k,t_z}^{\mathrm{sl},-}$, while subject to the grid's DR requirements (P_{k,t_z}^{drr}). These findings, as the products of the actual implementation module, returned to DA to calculate the value of $P_{k,t_z,t'}^{\mathrm{sl},+}$, in equation (3), which are employed in the assessment of DR.

The linearly constrained nonlinear programming problem presented in equations (17)–(20) can be resolved through the interior-point technique [38]. From the customer's standpoint, the model's computation will determine the ideal amount of power restriction for both interruptible loads and shiftable loads, $P_{k,t_z}^{\mathrm{il},-}$ and $P_{k,t_z}^{\mathrm{sl},-}$, despite being bound by the grid's DR requirements (P_{k,t_z}^{drr}). The results obtained from the actual implementation module, serving as the outputs, will be sent back to demand analysis to calculate the value $P_{k,t_z,t'}^{\mathrm{sl},+}$ in equation (3). These values are employed to evaluate DR.

4.5 The outputs module

By integrating the impacts of LR and load reduction, one can calculate the overall request for a DR participant during the crisis, P^{E}_{k,t_z} can be derived accordingly as:

$$P^{\mathrm{E}}_{k,t_z} = P^{\mathrm{cl,rat}}_{k,t_z} + P^{\mathrm{il}}_{k,t_z} + P^{\mathrm{sl}}_{k,t_z} = \underbrace{P^{\mathrm{cl,rat}}_{k,t_z} + P^{\mathrm{il,rat}}_{k,t_z} + P^{\mathrm{sl,rat}}_{k,t_z}}_{\text{Outputs of demand analysis}} \underbrace{- P^{\mathrm{il},-}_{k,t_z} - P^{\mathrm{sl},-}_{k,t_z}}_{\text{Outputs of actual inplementation}} \underbrace{+ \sum_{t'=t_z-\delta_k}^{t_z-1} P^{\mathrm{sl},+}_{k,t' t_z}}_{\text{Outputs of demand analysis (dependent variable of actual inplementation outputs)}} \tag{21}$$

where $P^{\mathrm{cl,rat}}_{k,t_z}$ represents the power requirement of critical loads at a time-slot t_z.

In the work of this study, presuming that the system operator can have appliance-level knowledge regarding all its consumers $P^{\mathrm{cl,rat}}_{k,t_z}$, $P^{\mathrm{il,rat}}_{k,t_z}$ and $P^{\mathrm{sl,rat}}_{k,t_z}$ are deterministic values in equation (21).

4.6 Summaries

The aforementioned holistic framework possesses several superior and distinct hypothetical characteristics when compared to current DR modeling methods in the subsequent factors. Firstly, the suggested methodology considers inconsistencies in consumer activity during both the customer-specific and artificial intelligence phases, enabling it to account for the random variability of DR under multiple-timescales. This is as opposed to the majority of existing DR models [7, 18–24] which only consider uncertainties in DR on a short-term basis. Secondly, the presented contract selection model comprises an empirical component (Γ^{I}_{k}) and a learning-based component (Γ^{B}_{k}), allowing for the examination of both static and dynamic features in customers' DR decisions as they happen in real-life scenarios. Lastly, the suggested artificial intelligence (AI) artificial intelligence architecture integrates the benefits of both analytic and data-driven methods, enabling the identification of behavioral patterns for distinct customer segments without presuming their preferences. Thus, the composite model may prove to be a more pragmatic approach in real-world implementation than existing analytical approaches [26, 31].

5 Evaluation algorithm

5.1 Main procedures

This section evaluates the algorithm for quantifying DR's effect on renewable energy use in smart distribution grids, based on the metrics and DR model presented in Sections 2 and 3.

The evaluation flowchart can be seen in Figure 5.

A thorough description of all main steps can be seen below:

1. Input yearly time-series data for distributed renewable generation and system load demands.
2. For each interval, obtain a DR user's willingness factor by sampling from the probability distribution in Section 4. Consider customer load characteristics and willingness to determine the DR availability profile.
3. Perform optimal power flow analysis using the day-ahead scheduling model from Section 5.2. This model provides anticipatory dispatch based on day-ahead forecasts of renewable outputs and load demand.
4. Sample real-time renewable output and demand-side compliance based on forecast error and actual implementation models.
5. Using decisions from Step 3 and realizations from Step 4, perform immediate scheduling as per Section 5.3 to evaluate final dispatch considering day-ahead decisions and real-time uncertainties.
6. Determine renewable energy usage capacity and system operating cost in real-time.
7. Apply the RMP algorithm from Section 4 to update users' willingness probability distribution for the next interval.
8. Check if a new DR contractual interval has started. If so, resample new willingness factors for each DR user; otherwise, continue with the current factors.
9. Repeat Steps 3–7 until the simulation ends. Aggregate values for system evaluation indices, such as renewable penetration ratio and operating cost, for each period.

5.2 Day-ahead scheduling model

The day-ahead dispatch model focuses on minimizing the total operation cost of the distribution system, considering renewable energy and DR, including energy procurement, DR implementation, load shedding, and auxiliary services acquisition.

$$\underset{P^{\mathrm{drr}}_{k,t}, P^{\mathrm{usd}}_{k,t}, P^{w}_{j,t}, P^{pv}_{j,t}, P^{\mathrm{buy}}_{j,t}, P^{\mathrm{il,rat}}_{j,t}, P^{\mathrm{sl,rat}}_{j,t}}{\text{Minimize}} \sum_{j\in\Omega_F} \left(c_1 P^{\mathrm{buy}}_{j,t} + c_2 P^{a.+}_{j,t} + c_3 P^{a.-}_{j,t} + c_6 P^{\mathrm{drr}}_{j,t} + c_7 P^{\mathrm{usd}}_{j,t} \right). \tag{22}$$

The optimization is subject to several constraints including distribution network power flow, power balancing, DR availability, etc., as shown in equation (23)–(31):

$$P_{ij,t} = \sum_{(j,k)\in\Omega_F} P_{jk,t} + (P^{\mathrm{cl,rat}}_{j,t} + P^{\mathrm{il,rat}}_{j,t} + P^{\mathrm{sl,rat}}_{j,t} - P^{\mathrm{drr}}_{j,t}) - P^{\mathrm{usd}}_{j,t} - P^{w}_{j,t} - P^{pv}_{j,t} - P^{\mathrm{buy}}_{j,t} - P^{a.+}_{j,t} + P^{a.-}_{j,t}, \quad \forall (i,j)\in\Omega_F, \forall t \tag{23}$$

$$Q_{ij,t} = \sum_{(j,k)\in\Omega_F} Q_{jk,t} + \left(Q^{\mathrm{cl,rat}}_{j,t} + Q^{\mathrm{il,rat}}_{j,t} + Q^{\mathrm{sl,rat}}_{j,t} - Q^{\mathrm{drr}}_{j,t} \right) - Q^{\mathrm{usd}}_{j,t}, \quad \forall (i,j)\in\Omega_F, \forall t \tag{24}$$

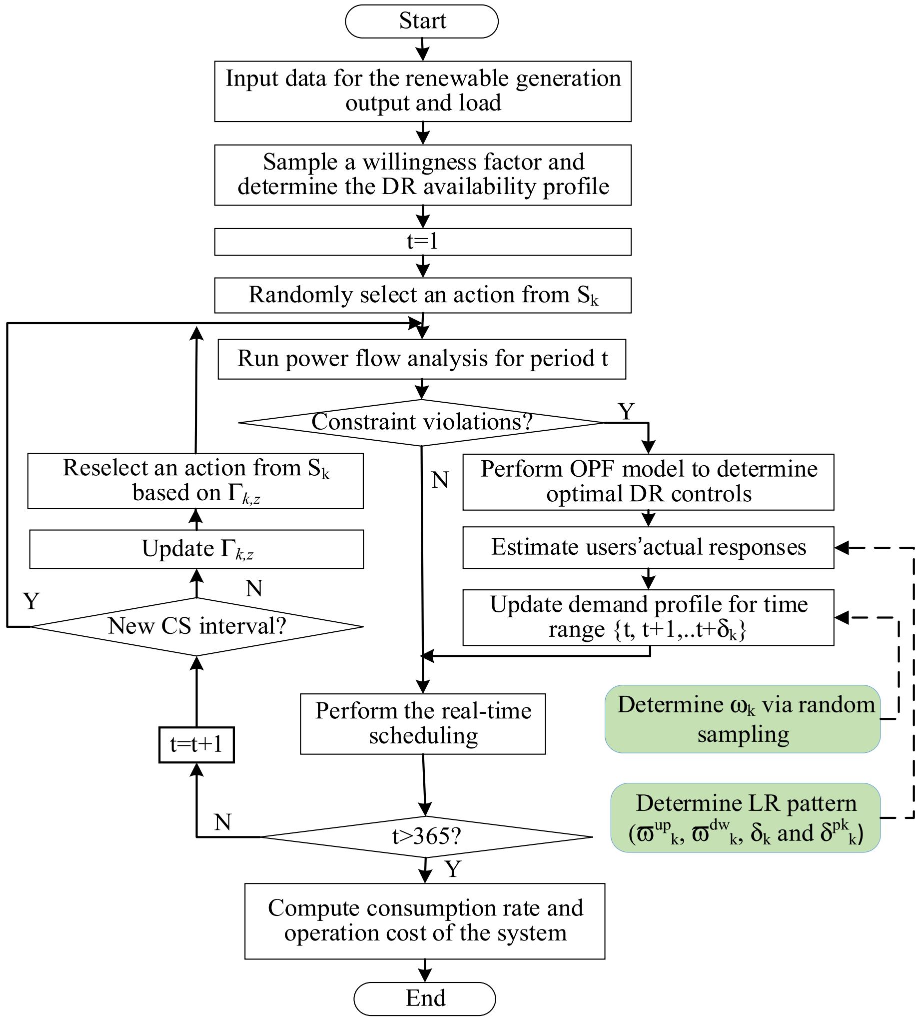

Fig. 5. Flowchart of the evaluation algorithm.

$$V_{i,t} = V_{j,t} + \frac{r_{ij}P_{ij,t}+\chi_{ij}Q_{ij,t}}{V_{0,t}} \quad \forall ij, t \tag{25}$$

$$I_{ij} = (V_{i,t} - V_{j,t})/\imath_{ij} \quad \forall (i,j) \in \mathbf{\Omega}_F, \forall t \tag{26}$$

$$V_{\min} \le V_{i,t} \le V_{\max} \quad \forall i, t \tag{27}$$

$$0 \le I_{ij,t} \le I_{ij,\max} \quad \forall (i,j) \in \mathbf{\Omega}_F, \forall t \tag{28}$$

$$P^{w}_{j,t} + P^{w.ab}_{j,t} = P^{w.act}_{j,t} \tag{29}$$

$$P^{pv}_{j,t} + P^{pv.ab}_{j,t} = P^{pv.act}_{j,t} \tag{30}$$

$$0 \le P^{\mathrm{drr}}_{k,t} \le P^{\mathrm{il,rat}}_{k,t} + P^{\mathrm{sl,rat}}_{k,t} \quad \forall k \in \mathbf{\Omega}_D, \forall t \tag{31}$$

$$0 \le P^{\mathrm{usd}}_{k,t} \le P^{\mathrm{cl,rat}}_{k,t} \quad \forall k \in \mathbf{\Omega}_D, \forall t. \tag{32}$$

Equations (23)–(24) are linearized power flow equations for distribution networks. To ensure the security of the system, equations (25)–(28) enforce constraints on the nodal voltage deviation and current-carrying capacity of feeder lines. Equations (29)–(30) represent the power output constraints of renewable energy generation, i.e., the available output is the additions of the actual power utilized and the abandoned power. Equations (31) and (32) specify the constraints on the maximum scheduling level and power shedding for each load node.

In these constraints, c_6 is the cost of demand reduction, c_7 is the penalty cost of lost load; $P^{\mathrm{usd}}_{k,t}$ and $Q^{\mathrm{usd}}_{k,t}$ denote the unsatisfied active/reactive load demand at node k in time t; $V_{i,t} = V_{j,t} + (r_{ij}P_{ij} + \chi_{ij}Q_{ij,t})/V_{0,t}, \forall i, j, t$ and $Q^{gen}_{j,t}$ are the active/reactive power output of the generating unit at system node j for time t; $P_{ij,t}$, $Q_{ij,t}$, and $I_{ij,t}$ denote active/reactive currents and currents in the network branch ij; $P^{w}_{j,t}$ is the wind turbine output utilization at node j in time t; $P^{w.ab}_{j,t}$ is the corresponding wind turbine disposal power, and $P^{w.act}_{j,t}$ is the predicted available output of the wind turbine; $P^{pv}_{j,t}$ is the output utilization of the PV unit at node j in time t; $P^{pv.ab}_{j,t}$ is the corresponding PV power abandonment; $P^{pv.act}_{j,t}$ is the predicted available PV output; $\mathbf{\Omega}_F$ is the set of system nodes; $V_{i,t}$ and $V_{0,t}$ are the voltage amplitudes at system node i and the relaxation node in time t; r_{ij},

r_{ij} and $\imath_{ij}$ are the resistance, reactance, and impedance values of the feeder ij.

In the day-ahead dispatch, the model is solved using predicted load and renewable generation values to create a power purchase plan and determine each customer's DR dispatch capacity, considering demand-side behavior. These results are then used in the intraday real-time scheduling model. The real-time scheduling accounts for changes in demand responsiveness and errors in day-ahead renewable forecasts.

5.3 Intraday scheduling model

The intra-day dispatch aims to reduce the actual operating charges of the system within the day, based on the day-ahead scheduling, as shown in equation (33):

$$\underset{P^{\mathrm{drr}}_{k,t}, P^{\mathrm{usd}}_{k,t}, P^{w}_{j,t}, P^{pv}_{j,t}, P^{a.+}_{j,t}, P^{a.-}_{j,t}}{\text{Minimize}} \sum_{(j,k)\in\Omega_F} \left(c_1 P^{\mathrm{usd}}_{k,t} + c_4 P^{a'.+}_{j,t} + c_5 P^{a'.-}_{j,t} \right). \tag{33}$$

In intraday scheduling, the power purchase and DR scheduling capacity are fixed, so they are regarded as constants in intra-day scheduling. When solving the model, equations (23)–(24) in the day-ahead dispatch need to be replaced with equations (34)–(35), but the corresponding dispatch willingness of each node load, renewable energy unit output, and customer DR need to use the data of the new scenario as a substitute because of the difference between the actual and predicted values.

$$P_{ij,t} = \sum_{(j,k)\in\Omega_F} P'_{jk,t} + \omega_k (P^{\mathrm{cl,rat}}_{j,t} + P^{\mathrm{il,rat}}_{j,t} + P^{\mathrm{sl,rat}}_{j,t} - P^{\mathrm{drr}}_{j,t})$$

$$-P^{\mathrm{usd}}_{j,t} - P^{w'}_{j,t} - P^{pv'}_{j,t} - P^{\mathrm{buy}}_{j,t} - P^{a'.+}_{j,t} + P^{a'.-}_{j,t}, \quad \forall (i,j) \in \Omega_F, \forall t \tag{34}$$

$$Q_{ij,t} = \sum_{(j,k)\in\Omega_F} Q_{jk,t} + \omega_k (Q^{\mathrm{cl,rat}}_{j,t} + Q^{\mathrm{il,rat}}_{j,t} + Q^{\mathrm{sl,rat}}_{j,t} - Q^{\mathrm{drr}}_{j,t}) - Q^{\mathrm{usd}}_{j,t},$$

$$\forall (i,j) \in \Omega_F, \forall t \tag{35}$$

where $P_{ij,t}$ and $Q_{ij,t}$ denote active/reactive currents and currents in the network branch ij; Ω_F is the set of system nodes; $P'_{jk,t}$ is the actual value of node j load in t time; ω_k is the customer's willingness to participate in DR and takes the value of a random number between 0 and 1, $P^{w'}_{j,t}$ is the actual wind turbine output at node j in time t, and $P^{pv'}_{j,t}$ is the actual PV output at node j in time t; $P^{a'.+}_{j,t}$ is the upper reserve capacity purchased in the auxiliary service market for a node j at a time t in the intra-day dispatch, $P^{a'.-}_{j,t}$ is the lower reserve capacity purchased in the auxiliary service market for a node j at a time t in the intra-day dispatch, and c_4, c_5 are the cost factors of the upper and lower reserve capacities, respectively. For the remaining constraints, equations (23)–(28) and equations (31)–(32) remain unchanged, and equations (29)–(30) are replaced with the following:

$$P^{w'}_{j,t} + P^{w.ab'}_{j,t} = P^{w.act'}_{j,t} \tag{36}$$

$$P^{pv'}_{j,t} + P^{pv.ab'}_{j,t} = P^{pv.act'}_{j,t}. \tag{37}$$

The actual output value of renewable energy is used here to replace the original forecast value, where $P^{w'}_{j,t}$ is the capacity factor of wind power generation at a node j in a time t; $P^{w.ab'}_{j,t}$ is the curtailed power of wind power generation; $P^{w.act'}_{j,t}$ is the actual available output of wind power generation; $P^{pv'}_{j,t}$ is the output of the PV unit at node j in time t, $P^{pv.ab'}_{j,t}$ is the corresponding PV power abandonment; and $P^{pv.act'}_{j,t}$ is the actual available PV output.

The purchased power and DR capacity from day-ahead dispatch are used as prior parameters for intraday dispatch. The main difference between intraday and day-ahead scheduling lies in the random fluctuations of energy demand, renewable output, and customer participation in DR during actual operations. DR helps mitigate the impact of these discrepancies. Intraday scheduling focuses on addressing wind curtailment and load loss that may occur after day-ahead scheduling, using DR to reduce the economic impact of these issues.

6 Case study

This part first confirms the efficiency of the proposed DR structure. It then conducts case studies to demonstrate how the framework can evaluate renewable energy consumption capacity in DR. The problem is solved using MATLAB R2019b on an Intel Core i7-9700 3.0 GHz PC with 16 GB RAM.

6.1 Validation of proposed DR models

6.1.1 Actual implementation module

The actual implementation module suggested in this study is validated by collecting the data from an actual China based DR program. For this test, two customers that have different consumption behaviors were randomly chosen as qualified. As reported in [34], the total capacity of User 1 is 124.8 kW for critical loads, 38.4 kW for interruptible loads, and 28.8 kW for shiftable loads, while User 2 has corresponding capacities of 82.3 kW, 24.4 kW, and 18.3 kW, respectively.

Data samples from 180 instances over 2 years were collected for the customer's individual history DR data. Every sample is denoted as $P^{\mathrm{hdr}} = \{P^{\mathrm{drr}}, P^{\mathrm{il},-}, P^{\mathrm{sl},-}\}$, hat accounts the effectiveness of each person in each of the 180 DR events, which characterizes their historical performance. This program utilizes the motivation and punishment rates of \$0.18/kWh and \$0.25/kW [35]. The cost of power is denoted as ρ_k, is set at \$0.14/kWh [36].

To verify the proposed framework, the data is split into a training set and a validation set. The training set, consisting of 130 samples from 180 datasets, helps understand user behavior patterns and calculate the actual implementation model specifications. The remaining 50 samples form the validation set, which evaluates the model's goodness-of-fit.

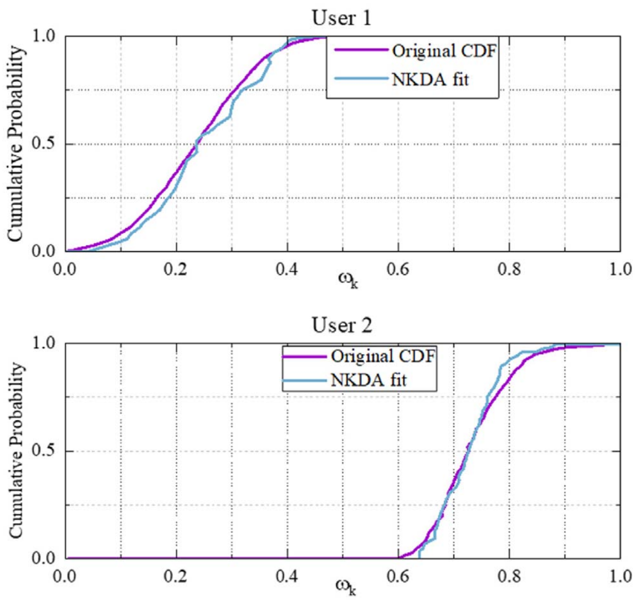

Fig. 6. Cumulative distribution functions for the training set's actual measurements and the predicted distribution model.

To optimize the nonparametric kernel density-based approach (NKDA), different kernel functions are analyzed, and an optimization method is applied to identify the optimal bandwidth. The mean-square-root error (MSRE) index is used to evaluate the fit. The kernel function with the lowest MSRE is chosen. The predicted outcomes from the NKDA are shown through the cumulative distribution function (CDF) in Figure 6.

It is evident that there is a significant level of consistency between the predicted and actual measurements in statistics for both customers, as evidenced by the relatively small area between the estimated and observed CDFs. To confirm this statistically, the widely-used chi-square (χ^2_∂) test is employed. This test measures the difference between the expected distribution and the actual samples using the χ^2_∂ statistic, with a smaller value indicating a higher level of accuracy in the prediction. If at a given significance level, the value of the test statistic χ^2_∂ is greater than the threshold value χ^2_∂ for that significance level, the distribution model's hypothesis will be disproved. Conversely, if the value of the test statistic is less than or equal to the threshold value, the model will be accepted [39]. Table 1 summarizes the χ^2_∂ statistic for the fitted $\psi(\omega_k)$ and this corresponding criterion value across various importance levels, as determined by the simulation.

6.1.2 Contract selection module

To create virtual data following a similar procedure as described in [40], a fuzzy logic technique tests the contract selection model. DR clients are categorized into empirical and learning-based users. Empirical users base their contract selection on propensities, while learning-based users consider preferences and DR profitability. Figure 7 and Table 2 display the membership algorithms and fuzzy logic rules for both customer categories.

Table 1. Chi-square analysis findings.

	χ^2 statistic	Threshold value			
		$\alpha = 0.1$	$\alpha = 0.05$	$\alpha = 0.01$	$\alpha = 0.005$
User 1	10.425	8.181	9.787	12.987	15.361
User 2	12.631				

Table 2. Fuzzy logic customer rules.

Rules	#1	#2	#3	#4	#5	#6	#7	#8	#9
Learning-based customers									
Regret	H	H	H	M	M	M	L	L	L
Preference	H	M	L	H	M	L	H	M	L
Fitness	H	LH	M	LH	M	LL	M	LL	L
Empirical-based customers									
Regret	H	H	H	M	M	M	L	L	L
Preference	H	M	L	H	M	L	H	M	L
Fitness	H	M	LL	H	M	L	LH	M	L

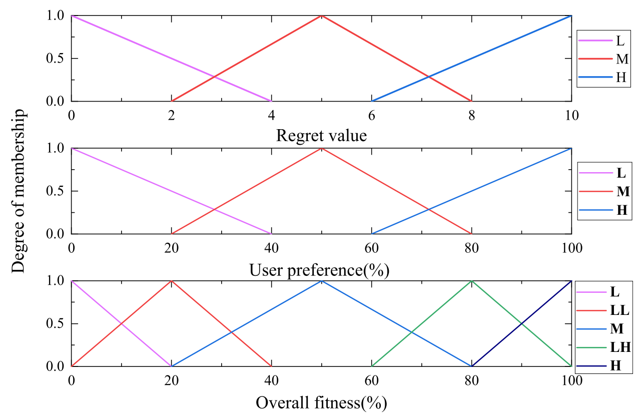

Fig. 7. Fuzzy membership functions.

The data used to create Figure 7 and Table 2 were gathered through 500 units taking part in a real commercial-based DR initiative in China distributed questionnaires. In Figure 7 and Table 2, L is used for low, M is used for middle, H is used for high, LL is used for little-low, and LH is used for little-high.

To conduct the test, 300 sets of chronological contract selection data were generated for both types of customers. The first 200 datasets determine the contract selection model's parameters, while the final 100 datasets are reserved for validation. The model's effectiveness is evaluated by comparing the observed data's first raw moment (mean) and second central moment (variance) with the predicted outcomes.

As depicted in Figure 8, the disparity in the mean and variance values is relatively negligible for both customer categories within the relevant time intervals. These findings suggest that the model's estimation closely aligns with the observed data, demonstrating good statistical consistency.

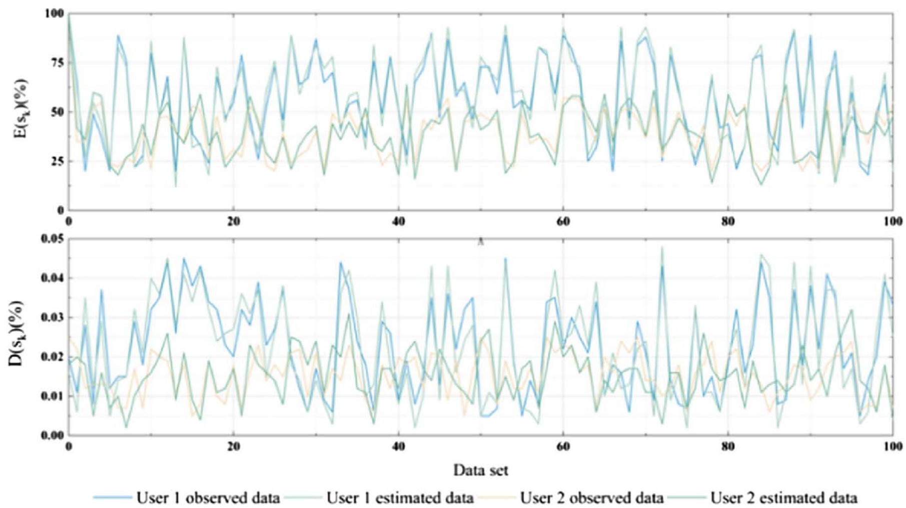

Fig. 8. Comparing the estimated and observed data, we asses $E(s_k)$ and $D(s_k)$.

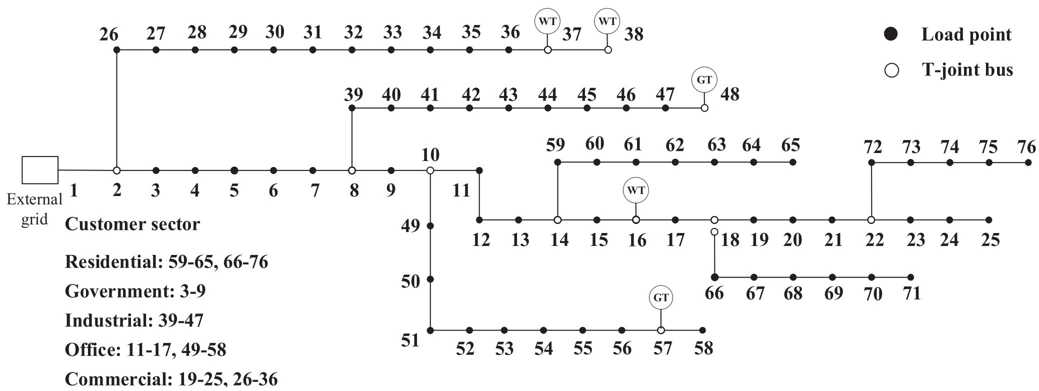

Fig. 9. A real regional distribution system.

Hence, it can be concluded that the proposed contract selection model effectively represents DR customers with diverse behavioral patterns in real-world settings.

6.2 Result analysis

6.2.1 Parameter settings

To confirm the efficacy of the suggested approach in a real smart-grid case with excess components, this section performs a numerical investigation on an actual distribution system.

The case study uses a real 10 kV regional distribution network in Beijing, with 64 load buses, 75 transmission lines, 2 gas turbines, and 3 wind farms, as shown in Figure 9. Customers are categorized as small industrial, commercial, residential, office building, and government based on their load patterns, with an annual peak load of 23.3 MW. Table 3 provides load information for each customer type. The energy reward, capacity reward, and penalty rate are set at \$0.18/kWh, \$0.45/kW, and \$0.25/kWh, respectively.

To demonstrate the advantage of the proposed approach, the renewable energy consumption rate and grid operation cost are compared across four different modeling scenarios. This study shows how the proposed methodology enhances renewable energy consumption and minimizes grid operation costs in real engineering applications.

6.2.2 Comparison with existing DR models

Multiple scenarios were set for comparison based on different DR uncertainties, renewable energy unit capacities, and DR types. The renewable energy consumption rate and operating costs were calculated for each scenario using numerical examples, demonstrating the efficiency of the proposed method.

The role of DR in the power grid can be used to absorb the differences in load differences caused by uncertainty that affects the original power generation plan of the grid, while DR itself also has uncertainty. When DR users are unwilling to participate in the system scheduling according to the original contract, it will have a certain negative impact on the operation of the system. To this end,

Table 3. Statistical data about system load demand.

	AAPR (%)	CRSD (%)	AVPR (%)	PCL (%)	PIL (%)	PSL (%)
Res.	42.21–58.74	34.85–44.93	88.24–92.35	75.23–87.63	3.82–8.56	9.43–15.64
Gov.	51.45–58.67	32.69–36.33	82.25–87.19	92.24–96.37	1.14–2.34	2.64–5.61
Ind.	85.13–90.22	17.32–21.46	60.12–67.35	52.34–76.25	8.43–19.31	15.13–27.15
Off.	67.73–71.22	35.39–40.43	75.11–80.37	77.44–87.24	4.41–9.49	7.55–12.47
Com.	72.40–78.51	27.45–33.42	51.64–56.44	78.14–83.33	6.20–12.22	9.27–17.94

AAPR: annual average-to-peak ratio; CRSD: corrected rational standard deviation (standard deviation × 100%/peak value); AVPR: annual valley-to-peak ratio; PCL: percentage of critical load in the total load demand; PIL: percentage of critical load in the total load demand; PSL: percentage of shiftable loads in the total load demand.

considering DR uncertainty, a comprehensive evaluation of DR benefits under the following four scenarios was conducted by assuming that long-term and short-term uncertainties exist or do not exist in the system.

Scenario 1:The modeling of DR in this study employs a fully deterministic approach, akin to previous works [8–10] and [19–21]. This entails treating the DR capacity of customers, as well as their observance amidst operation, as fixed variables.

Scenario 2: The DR model utilized in this study takes into account solely long-term uncertainties. Under this framework, customers' compliance during operation is presumed to be constant, while their DR participation level is regarded as a stochastic variable that aligns with the proposed contract selection model.

Scenario 3: The DR model adopted in this study focuses on short-term uncertainties, as in previous works [7] and [22–24]. Here, customers' participation level in DR is considered to be constant, whereas their operational performance is viewed as a stochastic variable that aligns with the proposed actual implementation model.

Scenario 4: Proposed DR model.

Let the equivalent load be the sum of the system load and DR load, then the equivalent load curve in each scenario can be obtained based on the model suggested in this study, as illustrated in Figure 10.

The renewable energy consumption and system operation cost under each scenario is reported in Table 4.

When using a deterministic and single time scale DR model, the system cost is lower, and the renewable energy consumption rate is higher. This indicates that DR's internal attributes largely offset the benefits of load redistribution, and system costs increase with higher uncertainty. Not accounting for long-term or short-term DR uncertainty may lead to overestimating renewable energy consumption capacity compared to the proposed case. Higher absorption rates correlate with lower total costs, showing that demand-side response can optimize the power structure, improve renewable energy absorption, and reduce electricity purchase costs. Considering uncertainty reduces renewable energy utilization rates and increases operating costs but provides more accurate decision-making for system operators, reducing economic losses from decision errors. Therefore, reliable modeling of these uncertainties is essential for a comprehensive assessment of renewable energy consumption potential. Underestimating DR's contribution

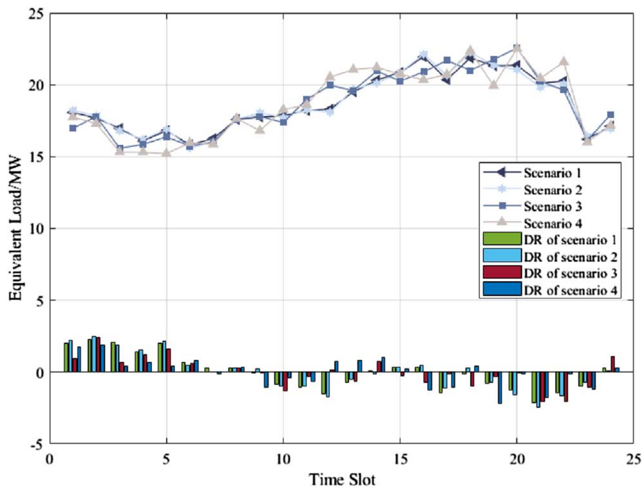

Fig. 10. Equivalent load curve in scenarios 1–4.

could lead to poor strategic planning, highlighting the advantages of the proposed comprehensive modeling framework over existing approaches.

6.2.3 Benefits of DR under different power supply structures

The main role of DR in the grid is to encourage the local consumption of renewable energy and reduce pollution emissions from power generation. In the actual grid system, considering that both PV units and wind turbines may be connected to the grid as renewable energy sources and there are certain differences in their generation characteristics, the power supply structure and its spatial and temporal matching with the load will have some impact on the benefits of DR.

Given this, this section examines the factors to elaborate on the optimal combination mechanism of distributed energy and DR in the distribution network. A comprehensive evaluation of DR benefits was performed under short-term uncertainty across four scenarios, considering the presence or absence of DR load in the system.

Scenario 5: The system contains 4 MW of rigid load, which does not participate in DR, and the renewable energy generation consists only of PV units.

Table 4. Renewable energy consumption rate and system operation cost under scenarios 1–4.

	Scenario 1	Scenario 2	Scenario 3	Scenario 4
Renewable energy consumption rate/%	77.98	75.31	74.23	71.06
System operation costs/10^5 $	20.49	24.28	21.45	27.86

Scenario 6: The system contains 4 MW of rigid load, which does not participate in DR, and the renewable energy generation consists only of wind turbines.

Scenario 7: The system contains 4 MW of DR load, and the renewable energy generation consists only of PV units.

Scenario 8: The system contains 4 MW of DR load, and the renewable energy generation consists only of wind turbines.

The equivalent load curve in all four scenarios can be obtained by solving the four scenarios using the model suggested in this research, as illustrated in Figure 11.

As seen in Figure 11 and Table 5, comparing scenarios 5 and 6 without considering DR, scenarios 7 and 8 with DR exhibit more significant peak shaving and valley filling characteristics under the same load. Under similar load response characteristics and capacity, DR's contribution to the distribution system is higher with wind power than with photovoltaic conditions. This is primarily due to wind power's anti-load regulation characteristics. At high penetration rates, the mismatch between generation and consumption times leads to excess wind power that cannot be fully consumed within several hours. Introducing the DR scheme adjusts the load curve, effectively increasing DR during low consumption periods, maximizing renewable energy use, and producing significant economic and environmental benefits.

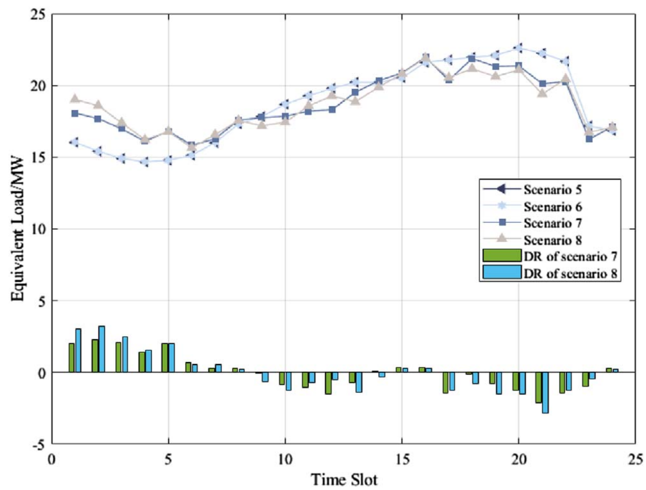

Fig. 11. Equivalent load curve in scenario 5–8. The renewable energy consumption and system operation cost under each scenario is presented in Table 5.

6.3 Impact of load composition on DR benefits

Combining the above analysis with the actual situation of the renewable energy distribution system, the differences in physical form and individual usage habits on the load side result in diverse customer responsiveness and response characteristics, directly impacting DR benefits.

In addition to the classification methods mentioned earlier, demand-side resources can also be categorized into three types from a DR participation perspective: interruptible load, shiftable load, and two-way interactive load. Interruptible loads can have their electricity consumption partially or fully curtailed as needed, such as air conditioning and large laundry facilities. Shiftable loads have a fixed total electricity consumption over a period but can adjust consumption flexibly within that period, including ice storage and industrial loads with independent production plans. Two-way interactive loads can interact with the grid in both directions, such as distributed energy storage and electric vehicles with V2G capabilities.

Combined with the proposed methodology, to study the role of the above factors, three scenarios are set as follows:

Scenario 9: Without interruptible load and shiftable load.

Scenario 10: All loads are shiftable loads.

Scenario 11: With two-way interactive load (containing both interruptible load and shiftable load, each accounting for 50%).

Assuming a consistent load capacity of 4 MW across all scenarios. Based on the proposed methodology, the DR benefits under these three scenarios are comprehensively analyzed and evaluated.

The equivalent load curve in each scenario was obtained based on the model suggested in this study, as shown in Figure 12.

At this time, the renewable energy consumption rate and system operation cost for each scenario are reported in Table 6.

The results in Figure 12 and Table 6 show that a system containing both interruptible and shiftable loads provides greater combined benefits to the renewable energy distribution network for a fixed total capacity. The evaluation index calculations indicate that different types of DR resources contribute differently to system efficiency. Compared to scenario 9, scenario 10 performs better in both evaluation indexes due to shiftable loads enhancing system flexibility, improving the distribution network's ability to handle emergencies, and increasing stability, thus reducing financial costs from severe accidents. Additionally, shiftable loads make fuller use of renewable energy, reducing wind and solar curtailment. Therefore, the reasonable use of shiftable loads helps improve the economy of renewable energy distribution network operations and supports low-carbon system operations. Scenario 11 further excels in both indicators compared to scenario 10. This improvement arises from the simultaneous consideration of shiftable and interruptible loads,

Table 5. Renewable energy consumption rate and system operation cost under scenarios 5–8.

	Scenario 5	Scenario 6	Scenario 7	Scenario 8
Renewable energy consumption rate/%	76.78	64.71	81.69	88.94
System operation costs/10^5 $	24.87	25.01	24.53	24.18

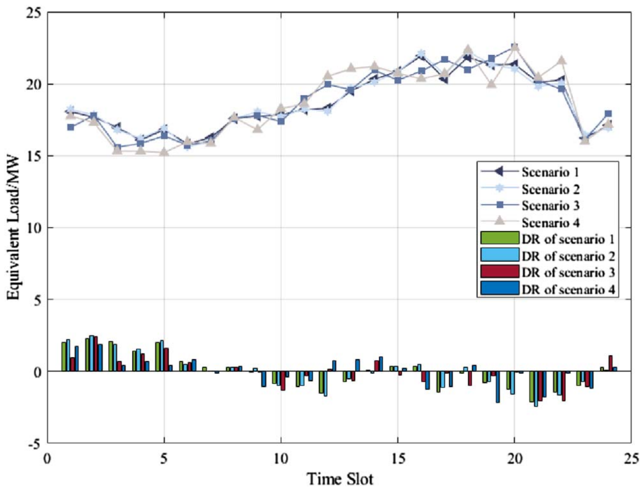

Fig. 12. Equivalent load curve in scenario 9–11.

Table 6. Renewable energy consumption rate and system operation cost under scenarios 9–11.

	Scenario 9	Scenario 10	Scenario 11
Renewable energy consumption rate/%	64.71	78.02	81.77
System operation costs/10^5 $	25.01	24.48	23.84

enhancing the economic operation of the system and unlocking DR's potential to contribute to the economic and environmental aspects of distribution network operations.

7 Conclusions

7.1 Concluding remarks

This paper constructs a model addressing the uncertainty of long-term contract selection and short-term load fluctuations in DR. It proposes an evaluation framework for quantifying DR involvement in renewable energy exploitation, systematically considering various demand-side uncertainties at different timescales. The primary conclusions are summarized below:

1. Considering the actual uncertainty of DR reduces the renewable energy consumption rate and increases total costs. Case studies show that accounting for uncertainty leads to an 8.87% reduction in renewable energy utilization and a 26.45% increase in operating costs. However, modeling this uncertainty improves decision-making accuracy.
2. In different renewable energy unit structures, DR has a greater impact on enhancing renewable energy consumption, particularly in systems with substantial shares of wind power and photovoltaics. This is primarily due to DR's ability to counteract load fluctuations. due to its anti-load regulation characteristics. Case studies show that with the installation of photovoltaic and wind power in the system, the presence of DR can increase the renewable energy consumption rate by 6.39% and 37.44%, respectively.
3. Different types of DR loads enhance the absorption rate of renewable energy, with multiple DR loads having a more significant effect. Case study results show that when DR is a shiftable load and a two-way interactive load, the renewable energy consumption rate increases by 20.57% and 26.35%, respectively, and the system operating cost decreases by 2.12% and 4.68%.

7.2 Limitations and future directions

Under the quantitative framework established in this paper, some challenges in studying DR uncertainty characterization and coordinated operation have been addressed. Although significant progress has been made, the future application of DR in power grids still faces many unresolved potential issues.

The research content of this paper also has a number of limitations, as follows:

1. Since DR involves the active response of many users, such responses may lead to false information reporting or irrational behaviors, raising doubts about data authenticity. This paper does not address the quality issue of system data.
2. For simplicity, this study relaxes the power flow constraints for the distribution system, which may reduce the practicability of the research to some extent.

Based on this, future research works may focus on the following aspects:

1. For DR characterization, it is essential to consider the impact of data quality in modeling demand-side behaviors to improve the model's effectiveness.
2. In future studies, the impacts of uncertainty factors, such as the authenticity and characteristics of data sources, should be considered to make the model formulation align more closely with practical cases.

Funding

This work was supported by the *State Grid Shanxi Electric Power Company Science and Technology* Project (520533220006).

Conflicts of interest

The authors declared no potential conflicts of interest with respect to the research, authorship, and/or publication of this article.

Data availability statement

The datasets used and/or analyzed during the current study are available from the corresponding author on reasonable request.

References

1 Mohammad Esmaeil H., Vahid H., Barry H., Miadreza S., Pierluigi S. (2021) An overview of demand response: from its origins to the smart energy community, *IEEE Access* **9**, 96851–96876.
2 Zhou Y.K. (2023) Sustainable energy sharing districts with electrochemical battery degradation in design, planning, operation and multi-objective optimisation, *Renew. Energy* **202**, 1324–1341.
3 Zhou Y.K., Lund P.D. (2023) Peer-to-peer energy sharing and trading of renewable energy in smart communities – trading pricing models, decision-making and agent-based collaboration, *Renew. Energy* **207**, 177–193.
4 Tang D., Fang Y.P., Zio E. (2023) Vulnerability analysis of demand-response with renewable energy integration in smart grids to cyber attacks and online detection methods, *Reliab. Eng. Syst. Saf.* **235**, 109212.
5 Jordehi A.R. (2019) Optimisation of demand response in electric power systems, a review, *Renew. Sustain. Energy Rev.* **103**, 308–319.
6 Li Y.C., Wang J.K., Zhang Y., Han Y.H. (2022) Day-ahead scheduling strategy for integrated heating and power system with high wind power penetration and integrated demand response: a hybrid stochastic/interval approach, *Energy* **253**, 124189.
7 Salehimehr S., Behrooz T., Mostafa S. (2022) Short-term load forecasting in smart grids using artificial intelligence methods: A survey, *J. Eng.* **12**, 1133–1142.
8 Norouzi F., Karimi H., Jadid S. (2023) Stochastic electrical, thermal, cooling, water, and hydrogen management of integrated energy systems considering energy storage systems and demand response programs, *J. Energy Storage* **72**, 108310.
9 Guo Z., Li G.Y., Zhou M., Li Z.F. (2018) Optimal operation of energy hub in business park considering integrated demand response, *Power Syst. Technol.* **42**, 8, 2439–2448. (In Chinese).
10 Wang L.Y., Lin J.L., Dong H.Q., Wang Y.Q., Zeng M. (2023) Demand response comprehensive incentive mechanism-based multi-time scale optimization scheduling for park integrated energy system, *Energy* **270**, 126893.
11 Singh B., Kumar A. (2023) Optimal energy management and feasibility analysis of hybrid renewable energy sources with BESS and impact of electric vehicle load with demand response program, *Energy* **278**, 127867.
12 Zhou Y.K. (2022) Demand response flexibility with synergies on passive PCM walls, BIPVs, and active air-conditioning system in a subtropical climate, *Renew. Energy* **199**, 204–225.
13 Zhou Y.K., Zheng S.Q. (2020) Machine-learning based hybrid demand-side controller for high-rise office buildings with high energy flexibilities, *Appl. Energy* **262**, 114416.
14 Zhou Y.K. (2022) Ocean energy applications for coastal communities with artificial intelligence – a state-of-the-art review, *Energy AI* **10**, 100189.
15 Liang W., Li H., Zhan S., Chong A., Hong T. (2024) Energy flexibility quantification of a tropical net-zero office building using physically consistent neural network-based model predictive control, *Adv. Appl. Energy* **14**, 100167.
16 Zhou Y.K. (2022) Demand response flexibility with synergies on passive PCM walls, BIPVs, and active air-conditioning system in a subtropical climate, *Renew. Energy* **199**, 204–225.
17 Zhou Y.K. (2022) Low-carbon transition in smart city with sustainable airport energy ecosystems and hydrogen-based renewable-grid-storage-flexibility, *Energy Rev.* **1**, 1, 100001.
18 Ahmed H.Y., AboRas M.K., Kotb H. (2023) A novel ultra local based-fuzzy PIDF controller for frequency regulation of a hybrid microgrid system with high renewable energy penetration and storage devices, *Processes* **11**, 4, 1093.
19 Mehdi N., Babak M. (2014) Reliability assessment of incentive- and priced-based demand response programs in restructured power systems, *Int. J. Elect. Power Energy Syst.* **56**, 3, 83–96.
20 Zhu J. (2023) Capacity optimization method of electrochemical energy storage system based on demand side response improved particle swarm optimization algorithm, *J. Phys. Conf. Ser.* **2418**, 1, 012099.
21 Li Y.T., Wang X.J. (2022) Community integrated energy system multi-energy transaction decision considering user interaction, *Processes* **10**, 9, 1794.
22 Yang K., Zhao Z.Y., Yu Y.J. (2022) Comprehensive evaluation of power system flexible resource value based on typical application scenarios, in: Zhang X., Ren H., Lu Y., Wang C. (Eds.), *Proc. GEESD*, IOS Press, pp. 176–182. https://ebooks.iospress.nl/doi/10.3233/ATDE220279.
23 Amirhos B., Hamidreza A., Somayeh M. (2022) Day-ahead optimal scheduling of microgrid with considering demand side management under uncertainty, *Electr. Power Syst. Res.* **209**, 107965.
24 Shankar P., Maurya R. (2023) Integration of solar powered DC homes to DC microgrid using dual active bridge converter, *Int. J. Power Electron.* **18**, 2, 163–175.
25 Zhou Y.K., Lund P.D. (2023) Peer-to-peer energy sharing and trading of renewable energy in smart communities – trading pricing models, decision-making and agent-based collaboration, *Renew. Energy* **207**, 177–193.
26 Yang H.J., Liu Z.K., Xie Y.X. (2023) A probabilistic liquefaction reliability evaluation system based on CatBoost-Bayesian considering uncertainty using CPT and Vs measurements, *Soil Dyn. Earthq. Eng.* **173**, 108101.
27 Pérez-Uresti S.I., Gallardo G., Varvarezos D.K. (2023) Strategic investment planning for the hydrogen economy – a mixed integer non-linear framework for the development and capacity expansion of hydrogen supply chain networks, *Comput. Chem. Eng.* **179**, 108412.
28 Luis G., António C., Zita V. (2022) Assessment of energy customer perception, willingness, and acceptance to participate in smart grids – a Portuguese Survey, *Energies* **16**, 1, 270–270.
29 Musa M.J., Hasan M.A., Sivaparthipan C. (2023) Future smart grids creation and dimensionality reduction with signal handling on smart grid using targeted projection, *Sustain. Comput. Inform. Syst.* **39**, 100897.
30 Hossein T., Mohammad Reza A., Luis B. (2022) Profit maximization for an electricity retailer using a novel customers' behavior leaning in a smart grid environment, *Energy Rep.* **8**, 908–915.
31 Jiang Z.H., Peng J.Q., Yin R.X., Hu M.M., Cao J.Y., Zou B. (2022) Stochastic modelling of flexible load characteristics of

split-type air conditioners using grey-box modeling and random forest method, *Energy Build.* **273**, 112370.

32 Zhang Y., Luo B., Cheng H. (2023) A multi-loads capacitive power transfer system for railway intelligent monitoring systems based on single relay plate, *Int. J. Circuit Theory Appl.* **52**, 1, 79–96.

33 Costa Vinicius B.F., Bonatto Benedito D., Silva Patrícia F. (2022) Optimizing Brazil's regulated electricity market in the context of time-of-use rates and prosumers with energy storage systems, *Uti. Policy* **79**, 101441.

34 Penizzotto F., Pringles R., Coria G. (2024) Valuation of investments in energy aggregator and storage systems by compound options, *Energy* **291**, 130458.

35 Zeng B., Wu G., Wang J.H., Zhang J.H., Zeng M. (2017) Impact of behavior-driven demand response on supply adequacy in smart distribution systems, *Appl. Energy* **202**, 125–137.

36 Balasubramanian S., Balachandra P. (2021) Effectiveness of demand response in achieving supply-demand matching in a renewables-dominated electricity system: a modeling approach, *Renew. Sustain. Energy Rev.* **147**, 111245.

37 Ontario Power Authority. *OPA demand response program* [Online]. Available at http://demand-response-shop.com/DR-brochure_Oct9.pdf (accessed: 2018.8.19).

38 Lu J. (2013) *Modern Consumer behavior*, Peking University Press, Beijing, China. (In Chinese).

39 Nolan S., Malley M.O. (2015) Challenges and barriers to demand response deployment and evaluation, *Appl. Energy* **152**, 1–10.

40 Hart S., Mas-Colell A. (2001) A reinforcement procedure leading to correlated equilibrium, in: Debreu G., Neuefeind W., Trockel W. (Eds.),*Economics essays*, Springer, Heidelberg, Berlin, Germany, pp. 181–200. https://link.springer.com/chapter/10.1007/978-3-662-04623-4_12.